[CANCER RESEARCH 63, 119–124, January 1, 2003]

Identification of Genes Responsible for Cell Migration by a Library of Randomized Ribozymes

Eigo Suyama, Hiroaki Kawasaki, Tatsuhiko Kasaoka, and Kazunari Taira[1]

Department of Chemistry and Biotechnology, School of Engineering, The University of Tokyo, Hongo, Tokyo 113-8656 [E. S., H. K., K. T.]; Gene Function Research Laboratory, National Institute of Advanced Industrial Science and Technology, Tsukuba Science City, Ibaraki 305-8562 [E. S., H. K., K. T.]; Tsukuba Research Institute, Novartis Pharma, Tsukuba Science City, Ibaraki 300-2611 [T. K.], Japan

ABSTRACT

Several genes appear to be associated with metastasis, but the underlying mechanisms of metastasis still remain unclear. In this study, we used a library of randomized ribozymes to identify, by inactivation of transcripts, genes involved in cell migration that is an essential aspect of metastasis. Using a chemotaxis assay, the ribozymes that inhibited cell migration were selected from the library. Among such ribozymes, we found two ribozymes that targeted and cleaved ROCK1 mRNA at independent sites. ROCK1 and ROCK2 are Rho kinases, and it has been demonstrated that they regulate the organization of the actin cytoskeleton and are responsible for cell motility and cytokinesis. The two ribozymes that specifically cleaved ROCK1 mRNA inhibited both the migration and invasion of invasive HT1080 fibrosarcoma, but neither had any effect on cell proliferation. Our analysis indicates that the ribozymes toward ROCK1 can block invasive activity but not the proliferation of HT1080 cells without having any effect on expression of ROCK2. Ribozymes identified in this study, including the ribozymes against ROCK1, might be useful in understanding the mechanisms of cell migration and metastasis.

INTRODUCTION

Metastasis is often one of the most serious problems for cancer therapy, and investigations of the mechanisms of metastasis have involved a variety of approaches (1–4). Comparisons, using DNA microarrays, of highly invasive and weakly invasive cancer cells have suggested that several genes are responsible for metastasis (5–7). There seems to be no doubt that DNA microarray analysis is a powerful tool for the diagnosis and basic research of cancer. However, microarray analysis does not reveal differences among activities of gene products; it only reveals differences in the levels of expression of particular genes (8). Therefore, to clarify the mechanisms of metastasis, a complementary technology is necessary that will allow us to correlate the activity of a gene product with a specific phenotype.

Ribozymes of various types have been used to interfere with the intracellular expression of specific genes via cleavage of the respective mRNAs (9–15). A well-characterized hammerhead ribozyme that consists of recognition arms at its 5′ and 3′ ends and a catalytic core region can bind to and cleave a substrate RNA (16). To create a ribozyme that specifically cleaves the transcript of a particular gene, the nucleotide sequences of the recognition arms are designed to be complementary to the sequence of the mRNA. When we randomize the sequences of the recognition arms, we can prepare a ribozyme library that is targeted to multiple mRNA substrates. Such a library can be used as a "knock down" library to interfere with the activities of numerous gene products (17–20). We can screen ribozymes and identify target genes that appear to be responsible for a particular phenotype by introducing such a ribozyme library into cells. Isolation of cells with the phenotype of interest allows the rescue of the ribozyme(s) of interest. Then, an examination of DNA databases allows rapid identification of the gene(s) responsible for the phenotype of interest using sequences of the rescued ribozyme(s).

Here, we describe the identification of genes responsible for migration and the isolation of ribozymes that would limit the expression of such genes using a library of randomized ribozymes. We focused on the motility of invasive cancer cells because the motility of strongly invasive cancer cells is known to be greater than that of noninvasive or weakly invasive cells, and also, motility is a prerequisite for metastasis (5, 21, 22). Indeed, inhibition of the motility of invasive cancer cells might be expected to prevent metastasis. For the selection of cells with defective migration using ribozymes, we chose a chemotaxis assay in a Boyden chamber (23). Cells that did not migrate toward the chemoattractant as a result of the effect of particular ribozymes were selected, and then ribozymes were isolated from such cells. The sequences of the recognition arms of these ribozymes were used to identify their targets. Among the selected ribozymes, we identified two ribozymes and determined that each cleaved the transcript of *ROCK1*, one of the genes that regulate the actin cytoskeleton (24, 25). The two ribozymes also inhibited the migration of and invasion by invasive HT1080 fibrosarcoma cells. Two related genes, *ROCK1* and *ROCK2*, are already demonstrated to be responsible for metastasis (26), and we found that *ROCK1* was responsible for motility but not for proliferation of HT1080 cells. Moreover, we identified genes other than *ROCK1* as candidates for the prevention of cell migration. The selected ribozymes and their alternative inhibitors against the candidate genes might be useful for cancer therapy.

MATERIALS AND METHODS

Construction of a Library of Randomized Ribozymes. Fragments of DNA that encoded randomized hammerhead ribozymes were generated by PCR with, as the template, 5′-TCC CCG GTT CGA AAC CGG GCA CTA CAA AAA CCA ACT TTN NNN NNN CTG ATG AGG CCG AAA GGC CGA AAN NNN NNG GTA CCC CGG ATA TCT TTT TTT-3′ and primers 5′-TCC CCG GTT CGA AAC CGG GCA-3′ (sense) and 5′-GCT TGC ATG CCT GCA GGT CGA CGC GAT AGA AAA AAA GAT ATC CGG GGT-3′ (antisense). The sequence of the template was based on a $tRNA^{Val}$-fused hammerhead ribozyme. Construction of the ribozyme expression vector based on a plasmid pPUR (Clontech, Palo Alto, CA) was performed as described previously (27, 28). The plasmid DNA carrying randomized ribozymes was introduced into competent bacteria, *Escherichia coli* DH5α (TOYOBO, Osaka, Japan), and 5×10^6 colonies of bacterial cells were obtained. Then, the plasmid DNA that harbored the ribozymes was purified from the transformants.

Culture and Transfection of Cells. HT1080 human fibrosarcoma cells and B16-BL6 mouse melanoma cells were kindly provided by Dr. Nakajima (Novartis Pharma Research Japan, Tsukuba, Japan). Cells were maintained in RPMI 1640 (Sigma Chemical Co., St. Louis, MO), supplemented with 10% fetal bovine serum and an antibiotics mixture (Life Technologies, Inc., Rockville, MD). Transfection of HT1080 cells was performed using a cationic transfection reagent, Trans-IT LT1 (Mirus, Madison, WI), according to the manufacturer's instructions. For examination of the results of transient transfections, cells were subjected to assays 24 h after transfection. Stable transfectants were selected by culture for 3 weeks in medium that contained puromycin (2.5 μg/ml).

Received 6/11/02; accepted 10/30/02.

The costs of publication of this article were defrayed in part by the payment of page charges. This article must therefore be hereby marked *advertisement* in accordance with 18 U.S.C. Section 1734 solely to indicate this fact.

[1] To whom requests for reprints should be addressed, at Department of Chemistry and Biotechnology, Graduate School of Engineering, The University of Tokyo, Hongo, Tokyo 113-8656, Japan. Phone: 81-3-5841-8828; Fax: 81-3-5841-8828; E-mail: taira@chembio.t.u-tokyo.ac.jp.

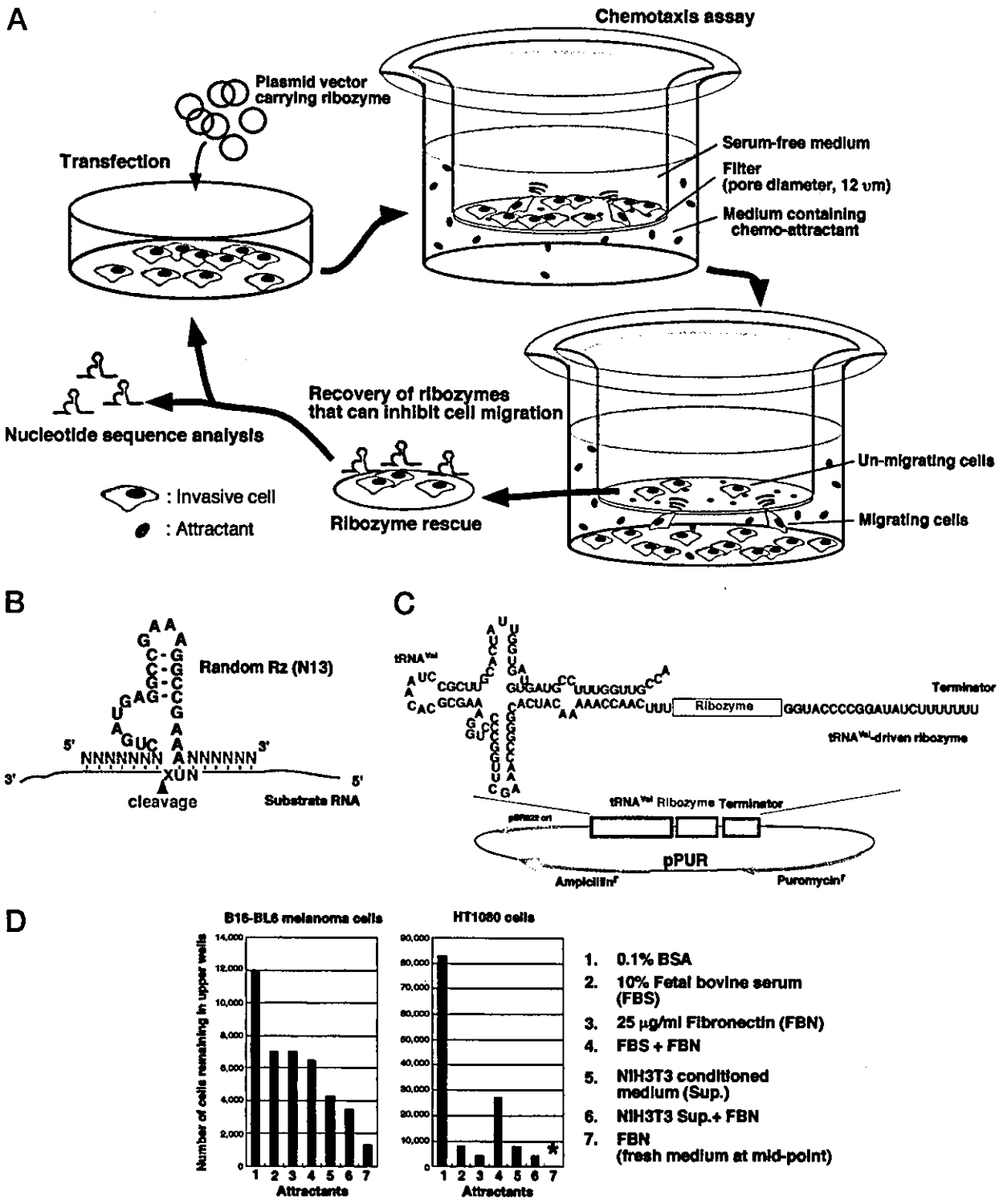

Fig. 1. Chemotaxis assay for gene discovery using randomized hammerhead ribozymes. *A*, schematic representation of the assay. In *B*, hammerhead ribozymes are catalytic RNA molecules that bind to target RNA molecules via Watson-Crick base pairing. They cleave their targets enzymatically. The recognition arms of the ribozyme library are randomized. The substrate RNAs should contain NUX triplet (where *N* and *X* represent A,U,G,C and A,U,C) for cleavage by hammerhead ribozymes (36, 37). In *C*, randomized ribozymes were cloned into the plasmid vector pPUR, which carries the promoter of a human gene for $tRNA^{Val}$. This RNA pol III-dependent expression system is suitable for expression of short RNAs, and ribozymes are expressed as $tRNA^{Val}$-fused RNAs (28). *D*, optimization of the chemotaxis assay. The numbers of cells remaining in the top well after a 24-h chemotaxis assay are indicated for each chemoattractant. Human HT1080 cells and mouse B16-BL6 melanoma cells were used as invasive cells. BSA was a negative control for chemoattractant. When we used fibronectin, fresh medium and removal of the migrating cells from the membrane at the midpoint of the assay reduced the number of cells remaining in the top well (*).

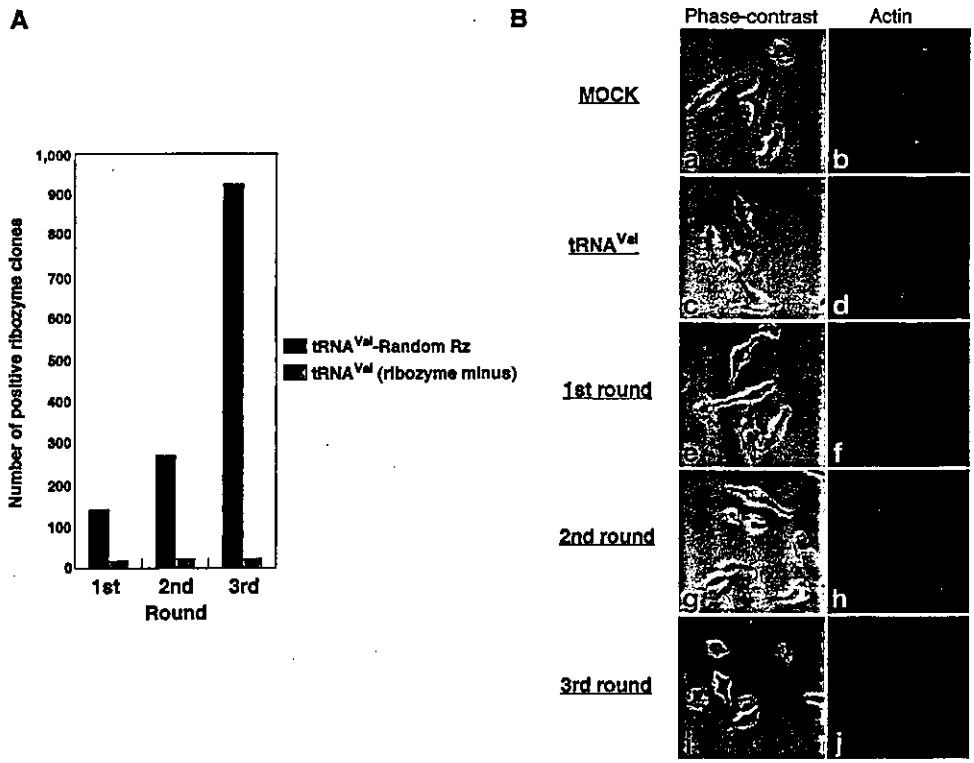

Fig. 2. Concentration of effective ribozymes. In *A*, the numbers of bacterial clones that harbored effective ribozymes obtained after the first, second, and third round of selection are indicated. The numbers increased from the first to third round of selection. In *B*, a similar effect on changes in morphology was also observed. Phase-contrast images of cells and fluorescent images of FITC-stained actin in cells are shown. In comparison with mock-transfected cells (*MOCK*; *a* and *b*) and cells transfected with the empty vector (*tRNA^{Val}*; *c* and *d*), shrunken-shaped cells increased in number gradually after transfection with the ribozyme library and number of rounds of selection (*e–j*).

Assays of Chemotaxis and Invasion. Cell migration assays were performed using 12-μm-pore Transwell inserts (Costar, Cambridge, MA). By contrast, 8-μm-pore inserts were used for confirmatory assays. Invasion assays were performed with a Cell Invasion Assay Kit (Chemicon, Temecula, CA) as described elsewhere (29). When cells reached 60–70% confluence, they were collected, washed twice with PBS, and suspended in RPMI 1640 plus 0.1% BSA (Sigma) at 2×10^5 cells/ml for assays of cell migration. We seeded 1×10^5 cells in each transwell insert and performed the invasion assay according to the manufacturer's instructions.

Plasmid Rescue. The recovery of plasmid DNA from cells that did not migrate to the bottom well was performed by alkaline lysis with SDS (Qiagen GmbH, Hilden, Germany). The resultant plasmid DNAs were introduced into competent *E. coli* DH5α cells. Colonies appearing on plates were counted and picked up for the determination of sequences of ribozymes.

Immunofluorescence Staining and Microscopy. To visualize the actin cytoskeleton, treated cells were rinsed with PBS and fixed with 3.7% formaldehyde in PBS for 30 min. Cells were rinsed again with PBS and then treated with 100% methanol at −20°C for 30 min. After washing with PBS, cells were labeled with a preparation of FITC-phalloidin (kindly provided by Dr. Nagasaki, Advanced Industrial Science and Technology, Tsukuba, Japan). Phase-contrast and fluorescent images were recorded with an LSM510-V2.01 system (Carl Zeiss, Jena, Germany).

Preparation and Analysis of Cell Extract. Cell lysates were prepared by lysing plated monolayers of cells with lysis buffer [10 mM Tris-HCl (pH 7.4), 150 mM NaCl, 5 mM EDTA, 1% Triton X-100, 0.1% SDS], supplemented with a protease inhibitor cocktail (Complete Mini; Roche Diagnostics GmbH, Mannheim, Germany) according to the manufacturer's instructions. Aliquots of 30 mg of total protein were fractionated on an SDS-polyacrylamide (7.5%) gel, and bands of protein were transferred to a polyvinylidene difluoride membrane (ATTO, Tokyo, Japan). Antibodies used were as follows: rabbit polyclonal antibodies against ROCK1, ROCK2, actin (all from Santa Cruz Biotechnology, Santa Cruz, CA), and horseradish peroxidase-linked antibodies against rabbit IgG raised in donkey (Amersham Pharmacia, Piscataway, NJ). Immunoreactive bands were detected with enhanced chemiluminescence plus reagent (Amersham Pharmacia) according to the manufacturer's instructions.

Assays of Cell Proliferation and Viability. Cells were seeded at 1×10^3 cells/well in 96-well optical bottom plates (Nalge Nunc, Rochester, NY). The proliferation and viability of cells were monitored in terms of luminescence with a CellTiter-Glo Assay kit (Promega, Madison, WI) and using a multilabel plate reader (Perkin-Elmer, Turku, Finland).

RESULTS

Identification of Ribozymes that Block Chemotaxis. For the isolation of ribozymes that can inhibit cell migration and identification of the respective target genes, we used the assay system shown in Fig. 1*A*. First, we treated highly invasive cancer cells with the library of randomized hammerhead ribozymes that had been constructed as shown in Fig. 1, *B* and *C*. The treated cells were then subjected to the chemotaxis assay. Most cells migrated toward the chemoattractant, moving from the top well to the bottom well, which contained the chemoattractant. Cells that did not migrate as a result of the inhibitory effects of ribozymes were collected from the top well, and ribozymes were recovered from these cells. The ribozymes that inhibited cell migration were sequenced to allow identification of the genes whose mRNAs had, apparently, bound to the ribozymes via Watson-Crick base pairing and had been cleaved (Fig. 1*B*) by a DNA sequence database search. A new population of cells was then subjected to the assay after introduction of the newly identified ribozymes to validate their effects.

Optimization of the Assay. In the assay shown in Fig. 1*A*, cells of interest might be mixed with cells that remain in the top well independently of the effects of ribozymes. We examined how many untreated cells remained in the top well during a 24-h assay, using invasive human fibrosarcoma HT1080 cells and mouse B16-BL6 melanoma cells. We tested fibronectin, fetal bovine serum, and conditioned medium from cultures of NIH3T3 cells as chemoattractants (23). HT1080 cells migrated more efficiently than B16-BL6 toward each chemoattractant (Fig. 1*D*). Moreover, replacement of the medium in the bottom well and removal of migrated cells from the membrane with a swab at the midpoint of the assay reduced the number of cells that remained in the top well (Fig. 1*D*, *right, column 7*). Because cells that had migrated to the bottom well could return to

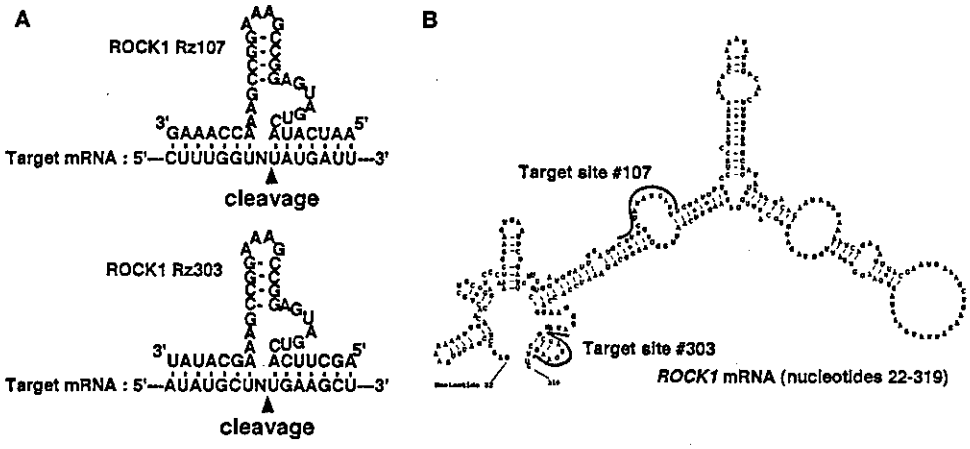

Fig. 3. Ribozymes that cleaved *ROCK1* mRNA. *A*, structures of the ribozymes (*Rz*) directed against *ROCK1* mRNA. The substrate RNA should contain a complementary sequence to that of recognition arms of the ribozyme. *B*, partial structure of ROCK1 mRNA (corresponding to nucleotides 22–319, according to the numbering in Ref. 24). *Gray lines*, target sites of the ribozymes. Prediction of RNA conformation was made with the mulfold program (http://iubio.bio.indiana.edu/molbio/mac/mulfold.hqx.) (38).

the top well by random migration known as chemokinesis (30), the removal of migrated cells at the midpoint of the assay might have reduced the number of nonmigrating cells recorded at the end of the assay. This was suitable for our purposes because of the very low background effect attributable to nonmigrating cells. All subsequent assays, therefore, were carried out under these conditions with HT1080 cells and fibronectin.

Recovery of Ribozymes from Nonmigrating Cells. HT1080 cells treated with a plasmid library of randomized ribozymes were subjected to the chemotaxis assay. After a 24-h incubation, we isolated plasmid DNA from nonmigrating cells that remained in the top well. We then introduced the isolated plasmid DNA directly into competent *E. coli* cells. The colonies that appeared after antibiotic selection were counted (Fig. 2*A*). Initially, 141 clones were isolated from cells that had been treated with the library of $tRNA^{Val}$-fused ribozymes [ribozyme (+)]. By contrast, only 20 clones were obtained after cells had been treated with $tRNA^{Val}$ expression plasmids that lacked a ribozyme sequence [ribozyme (−)], which we used as negative controls. The number of ribozyme (+) clones obtained in the assay increased during our confirmatory assays, and we obtained 924 clones in the third round of selection (Fig. 2*A*). The number of ribozyme (−) clones did not change significantly. Our results indicated that plasmids that encoded the active ribozymes could be selected in a chemotaxis assay. The assay also allowed us to concentrate these plasmid DNAs as the number of rounds of the assay increased.

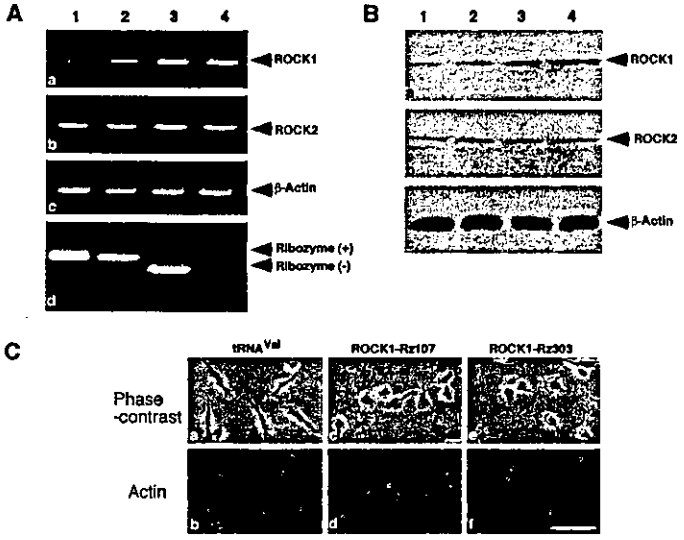

Fig. 4. Specific reductions in the level of expression of *ROCK1* by the selected ribozymes. Reduction in the level of expression of *ROCK1* was detected in cells that expressed the ribozymes toward *ROCK1* mRNA (ROCK1 ribozymes) by RT-PCR (*A*) and immunoblotting analysis (*B*). *Lanes 1* and *2*, cells that expressed ROCK1 ribozyme107 and ROCK1 ribozyme303; *Lane 3*, cells that expressed a plasmid that encoded only $tRNA^{Val}$ (empty vector); *Lane 4*, nontreated HT1080 cells. The expression of *ROCK2*, a homologue of *ROCK1*, was not affected by the two ribozymes (*A-b* and *B-b*). As internal controls for both analyses, results for β-actin are also shown (*A-c* and *B-c*). The expression of the ribozymes and control $tRNA^{Val}$ was also confirmed by RT-PCR (*A-d*). *C*, morphological changes of HT1080 cells by the ribozymes toward ROCK1. Cells treated with empty vector ($tRNA^{Val}$; *a* and *b*), ROCK1 ribozyme107 (*c* and *d*), or ROCK1 ribozyme303 (*e* and *f*). Transient expression of the ribozymes suppressed an elongated morphology of HT1080 cells. Scale bar, 100 μm.

Morphological Changes of Ribozyme-treated Cells. Cell migration is strictly regulated by reorganization of the actin cytoskeleton and focal adhesion (31, 32). Previous studies of metastasis revealed that strongly and weakly invasive cells differ in terms of morphology (5) and suggested that such differences might be attributable, at least in part, to differences in motile activity, in particular, the reorganization of the actin cytoskeleton, *e.g.*, the dominant-inhibitory Rho (one of the regulators of the actin cytoskeleton) mutant suppressed an elongated morphology of human A375 melanoma cells (5). Because reorganization of the actin cytoskeleton generates intracellular tension, invasive cells might tend to be more elongated than noninvasive cells. Thus, we postulate that such a morphological change can be one of the indicators of the changes in adhesiveness and the actin cytoskeleton. HT1080 cells are usually extended, long, and narrow, as were our wild-type cells and even the cells after transfection with the first ribozyme library (Fig. 2*B*). Cells that appeared somewhat shrunken were observed among elongated cells after transfection with the ribozymes selected in the first round. The population of shrunken cells was clearly greater after the third round of selection than after the first. These observations suggested ribozymes that inhibited cell migration were selected and concentrated as the number of selections increased.

Isolation of Ribozymes that Cleaved *ROCK1* mRNA and Their Effects. We isolated and sequenced the ribozymes obtained during the third round of selection. The sequences of the recognition arms of a ribozyme should be complementary to its specific substrate RNA, in this case, the mRNA that is responsible for cell migration. Among candidate ribozymes selected in our assay, we identified two independent ribozymes that apparently cleaved *ROCK1* mRNA at different sites (Fig. 3*A* and *B*). *ROCK1*, as the target gene of two ribozymes, was identified in human DNA databases using the BLAST program[2] with the parameters set automatically to optimize for searching with short sequences (search program for short nearly exact sequences) with the setting of EXPECT threshold = 100 and LIMITATION

[2] Internet address: http://www3.ncbi.nlm.nih.gov/BLAST/.

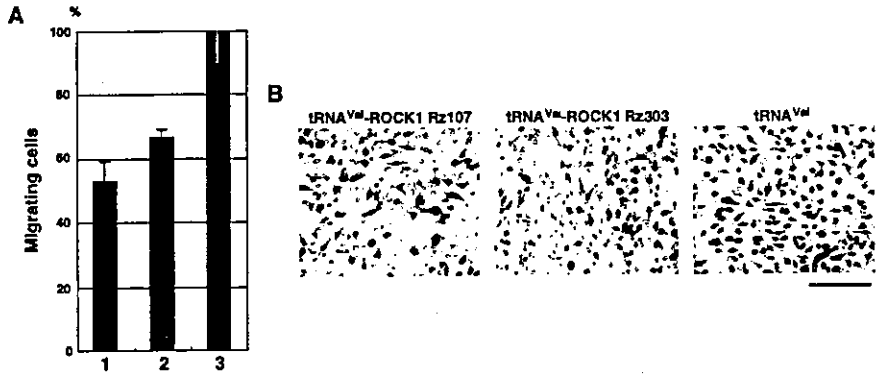

Fig. 5. Inhibition of cell migration by the ribozymes toward *ROCK1*. *A*, inhibition by ribozymes of migration was correlated with the presence of ribozyme-directed *ROCK1* mRNA. HT1080 cells that expressed ROCK1 ribozyme107, ROCK1 ribozyme303, or tRNA^{Val}, as a control, were allowed to migrate toward fibronectin for 24 h. In *B*, migrating cells on the microporous membrane were visualized by Giemsa staining. Scale bar, 200 μm.

terms; Homo sapiens and cds (coding DNA sequence). EXPECT threshold is a statistical parameter that regulates the stringency of the database search. As a result of searching with the parameter settings mentioned above, the sequences of the target of the ribozymes were not found in other expressed genes except *ROCK1*. ROCK is considered to be a regulator of the reorganization of the actin cytoskeleton (25). Therefore, it seems reasonable that our method allowed us to isolate and identify ribozymes that cleaved *ROCK1* mRNA.

Next we checked if the ribozymes toward *ROCK1* mRNA could indeed cleave *ROCK1* mRNA. An examination by RT-PCR[3] and immunoblotting analysis indicated clearly that the two ribozymes specifically cleaved *ROCK1* mRNA and reduced the level of expression of ROCK1 itself (Fig. 4*A* and *B*). The level of expression of the *ROCK2* gene, whose full-length nucleotide sequence is similar to that of *ROCK1*, did not decrease at all. The ribozymes toward *ROCK1* mRNA specifically recognized and cleaved their cognate substrate, *ROCK1* mRNA. Furthermore, we observed the effects of transient expression of the ribozymes toward ROCK1 on the morphology of HT1080 cells. As expected, the expression of the ribozymes led to morphological changes in the cells. The ribozymes suppressed the elongated morphology of HT1080 cells (Fig. 4*C*).

We also examined whether the two ribozymes were actually responsible for the nonmigratory phenotype of invasive HT1080 cells. As shown in Fig. 5*A* and *B*, chemotaxis assays confirmed that the ribozymes inhibited the migration of cells. Moreover, inhibition of cell migration by the ribozymes seemed to be correlated with reduction in the expression of *ROCK1* mRNA in cells. This result indicated the importance of *ROCK1* in cell motility.

Effects of the Ribozymes on Invasion and Cell Proliferation. The identified ribozymes toward *ROCK1* inhibited cell migration, but it was not clear that they would affect cell invasion. Invasion requires the migration of cells and the dissolution of the extracellular matrix (29). We postulated that the ribozymes that cleaved *ROCK1* mRNA should also inhibit cell invasion because they inhibited cell migration. As a result, not only did these ribozymes inhibit cell invasion (Fig. 6*A*), but the inhibition of cell invasion also seemed to be correlated with a reduction in the expression of *ROCK1*.

ROCK1 contributes to the reorganization of the actin cytoskeleton, and such a reorganization of actin is required both when cells migrate and when they undergo cytokinesis. Therefore, it is possible that ribozymes that cleave *ROCK1* mRNA might also inhibit proliferation. We found, however, no differences in terms of cell proliferation between ribozyme-treated and nontreated HT1080 cells (Fig. 6*B*). It is possible that migration might be more sensitive than cytokinesis to a reduction in the level of expression of the ROCK1 protein. Indeed, the ribozymes did not totally eliminate expression of *ROCK1* (Fig. 4). Moreover, several redundant pathways or proteins might exist to safeguard the essential processes of cytokinesis and proliferation.

DISCUSSION

To our knowledge, this study provides the first example of use of a chemotaxis assay and a library of randomized ribozymes to identify genes responsible for cell migration. We isolated two independent ribozymes that target *ROCK1* mRNA. As noted above, ROCK1 is one of the regulators of the actin cytoskeleton and appears to modulate signals for regulation of the actin cytoskeleton from Rho (a member of the Ras-related family of low molecular weight GTPases) through LIM kinase to cofilin, which can depolymerize actin filaments and reorganize the cytoskeleton (33). Ribozymes against *ROCK1* mRNA inhibited cell migration and invasion but did not affect cell proliferation. It remains to be determined whether regulation of the organization of actin by ROCK1 in cytokinesis is distinct from the role of ROCK1 in migration. In our preliminary study, a ribozyme toward LIM kinase inhibited cell migration but not proliferation of invasive HT1080 cells. Therefore, ROCK1 and LIM kinase might play important roles in cell migration but not in cytokinesis. In addition, we can postulate that ROCK1 is more important for cell migration than ROCK2 by the fact that we isolated ribozymes toward ROCK1 by the assay and that ribozymes toward ROCK2 were not identified. We plan to construct expression vectors for ribozymes toward ROCK2 and to investigate the effects of the ribozymes on cell migration and invasion. Additional investigations using ribozymes toward ROCK2 will

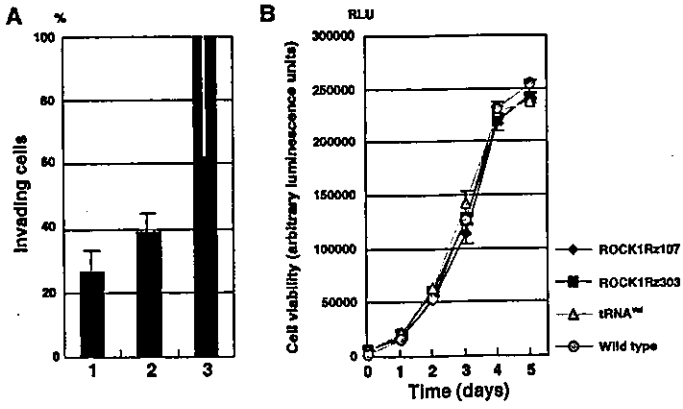

Fig. 6. The ribozymes inhibited invasion without any effect on proliferation. In *A*, ROCK1 also regulated invasion by HT1080 cells. Cells used in this assay were identical to those used in the chemotaxis assay for which results are shown in Fig. 4*A*. In *B*, cell proliferation (cell number) was monitored in terms of luminescence. ROCK1 ribozymes had no effect on cell proliferation and viability. Each *column* and *bar* represents the mean ± SD of results of three independent experiments performed in triplicate.

[3] The abbreviations used are: RT-PCR, reverse transcription-PCR.

clarify whether ROCK2 contributes to cell migration and whether ROCK1 and ROCK2 play separate and specialized roles or not. The Rho-ROCK system has been implicated in cell mobility, migration, and metastasis in a variety of cell types, *e.g.*, a specific ROCK inhibitor Y-27632 blocked the invasive activity of rat MM1 hepatoma cells (26). Therefore, we expect that the ROCK1 ribozymes may lead to the inhibition of cell migration in several cancer cell lines and that ribozymes and its alternative inhibitors targeted specifically to *ROCK1* mRNA might be useful in cancer therapy as low toxicity compounds that inhibit cell motility without affecting cell viability.

As noted above, migration requires regulation of the organization of the actin cytoskeleton. Indeed, using the chemotaxis assay, we isolated ribozymes against genes that are thought to encode proteins involved in the regulation of the organization of actin, such as ROCK1 as discussed above; myosin-IXb (34), which acts both as a motor protein and as a GTPase-activating protein for the Rho family; and adducin (35), which is a substrate for protein kinase C and a mediator of the reorganization of actin filaments. The genes for these proteins seem to be targets for inhibition of cell migration, which might lead to the inhibition of metastasis. We also isolated ribozymes whose target genes remain to be identified. Additional investigations of these ribozymes and their target genes should help us to understand more clearly the mechanisms of cell migration and metastasis.

ACKNOWLEDGMENTS

We thank Dr. Motowo Nakajima (Tsukuba Research Institute, Novartis Pharma, Tsukuba Science City, Japan) for providing HT1080 fibrosarcoma and B16 BL6 melanoma cell lines. We also thank Dr. Laura Nelson (Advanced Industrial Science and Technology, Tsukuba, Japan) for very helpful comments on this manuscript.

REFERENCES

1. Tannock, I. F., and Hill, R. P. (eds.). The Basic Science of Oncology, Ed. 3. New York: McGraw-Hill, 1998.
2. Liotta, L. A., Steeg, P. S., and Stetler-Stevenson, W. G. Cancer metastasis and angiogenesis: an imbalance of positive and negative regulation. Cell, *64:* 327–336, 1991.
3. Fidler, I. J., and Radinsky, R. Search for genes that suppress cancer metastasis. J. Natl. Cancer Inst. (Bethesda), *88:* 1700–1703, 1996.
4. Weyers, W., Euler, M., Diaz-Cascajo, C., Schill, W. B., and Bonczkowitz, M. Classification of cutaneous malignant melanoma: a reassessment of histopathologic criteria for the distinction of different types. Cancer (Phila.), *86:* 288–299, 1999.
5. Clark, E. A., Golub, T. R., Lander, E. S., and Hynes, R. O. Genomic analysis of metastasis reveals an essential role for RhoC. Nature (Lond.), *406:* 532–535, 2000.
6. Bittner, M., Meltzer, P., Chen, Y., Jiang, Y., Seftor, E., Hendrix, M., Radmacher, M., Simon, R., Yakhini, Z., Ben-Dor, A., Sampas, N., Dougherty, E., Wang, E., Marincola, F., Gooden, C., Lueders, J., Glatfelter, A., Pollock, P., Carpten, J., Gillanders, E., Leja, D., Dietrich, K., Beaudry, C., Berens, M., Alberts, D., Sondak, V., Hayward, N., and Trent, J. Molecular classification of cutaneous malignant melanoma by gene expression profiling. Nature, *406:* 536–540, 2000.
7. Hippo, Y., Yashiro, M., Ishii, M., Taniguchi, H., Tsutsumi, S., Hirakawa, K., Kodama, T., and Aburatani, H. Differential gene expression profiles of scirrhous gastric cancer cells with high metastatic potential to peritoneum or lymph nodes. Cancer Res., *61:* 889–895, 2001.
8. Ridley, A. Molecular switches in metastasis. Nature (Lond.), *406:* 466–467, 2000.
9. Kruger, K., Grabowski, P. J., Zaug, A. J., Sands, J., Gottschling, D. E., and Cech, T. R. Self-splicing RNA: autoexcision and autocyclization of the ribosomal RNA intervening sequence of Tetrahymena. Cell, *31:* 147–157, 1982.
10. Guerrier-Takada, C., and Altman, S. Catalytic activity of an RNA molecule prepared by transcription in vitro. Science (Wash. DC), *223:* 285–286, 1984.
11. Sarver, N., Cantin, E. M., Chang, P. S., Zaia, J. A., Ladne, P. A., Stephens, D. A., and Rossi, J. J. Ribozymes as potential anti-HIV-1 therapeutic agents. Science (Wash. DC), *247:* 1222–1225, 1990.
12. Ojawang, J. O., Hampel, A., Looney, D. J., Wong-Staal, F., and Rappaport, J. Inhibition of human immunodeficiency virus type 1 expression by a hairpin ribozyme. Proc. Natl. Acad. Sci. USA, *89:* 10802–10806, 1992.
13. Kawasaki, H., Eckner, R., Yao, T. P., Taira, K., Chiu, R., Livingston, D. M., and Yokoyama, K. K. Distinct roles of the co-activators p300 and CBP in retinoic-acid-induced F9-cell differentiation. Nature (Lond.), *393:* 284–289, 1998.
14. Gesteland, R. F., Cech, T. R., and Atkins, J. F. (eds.). The RNA World, Ed. 2. Cold Spring Harbor, NY: Cold Spring Harbor Laboratory, 1999.
15. Tanabe, T., Kuwabara, T., Warashina, M., Tani, K., Taira, K., and Asano, S. Oncogene inactivation in a mouse model. Nature (Lond.), *406:* 473–474, 2000.
16. Krupp, G., and Gaur, R. K. (eds.), RIBOZYME: Biochemistry and Biotechnology. Natick, MA: Eaton Publishing, 2000.
17. Kruger, M., Beger, C., Li, Q. X., Welch, P. J., Tritz, R., Leavitt, M., Barber, J. R., and Wong-Staal, F. Identification of eIF2Bgamma and eIF2gamma as cofactors of hepatitis C virus internal ribosome entry site-mediated translation using a functional genomics approach. Proc. Natl. Acad. Sci. USA, *97:* 8566–8571, 2000.
18. Beger, C., Pierce, L. N., Kruger, M., Marcusson, E. G., Robbins, J. M., Welcsh, P., Welch, P. J., Welte, K., King, M. C., Barber, J. R., and Wong-Staal, F. Identification of Id4 as a regulator of BRCA1 expression by using a ribozyme-library-based inverse genomics approach. Proc. Natl. Acad. Sci. USA, *98:* 130–135, 2001.
19. Kawasaki, H., Onuki, R., Suyama, E., and Taira, K. Identification of genes that function in the TNF-a-mediated apoptotic pathway using randomized hybrid ribozyme libraries. Nat. Biotechnol., *4:* 376–380, 2002.
20. Kawasaki, H., and Taira, K. Identification of genes by hybrid ribozymes that couple cleavage activity with the unwinding activity of an endogenous RNA helicase. EMBO J., *3:* 443–450, 2002.
21. Woodhouse, E. C., Chuaqui, R. F., and Liotta, L. A. General mechanisms of metastasis. Cancer (Phila.), *80:* 1529–1537, 1997.
22. Yoshioka, K., Matsumura, F., Akedo, H., and Itoh, K. Small GTP-binding protein Rho stimulates the actomyosin system, leading to invasion of tumor cells. J. Biol. Chem., *273:* 5146–5154, 1998.
23. Varani, J. Chemotaxis of metastatic tumor cells. Cancer Metastasis Rev., *1:* 17–28, 1982.
24. Nakagawa, O., Fujisawa, K., Ishizaki, T., Saito, Y., Nakao, K., and Narumiya, S. ROCK-I and ROCK-II, two isoforms of Rho-associated coiled-coil forming protein serine/threonine kinase in mice. FEBS Lett., *392:* 189–193, 1996.
25. Narumiya, S., Ishizaki, T., and Watanabe, N. Rho effectors and reorganization of actin cytoskeleton. FEBS Lett., *410:* 68–72, 1997.
26. Itoh, K., Yoshioka, K., Akedo, H., Uehata, M., Ishizaki, T., and Narumiya, S. An essential part for Rho-associated kinase in the transcellular invasion of tumor cells. Nat. Med., *5:* 221–225, 1999.
27. Koseki, S., Tanabe, T., Tani, K., Asano, S., Shioda, T., Nagai, Y., Shimada, T., Ohkawa, J., and Taira, K. Factors governing the activity in vivo of ribozymes transcribed by RNA polymerase III. J. Virol., *73:* 1868–1877, 1999.
28. Kato, Y., Kuwabara, T., Warashina, M., Toda, H., and Taira, K. Relationships between the activities in vitro and in vivo of various kinds of ribozyme and their intracellular localization in mammalian cells. J. Biol. Chem., *276:* 15378–15385, 2001.
29. Repesh, L. A. A new in vitro assay for quantitating tumor cell invasion. Invasion Metastasis, *9:* 192–208, 1989.
30. Armitage, J. P., and Lackie, J. M. (eds.). Biology of the Chemotactic Response. Cambridge, United Kingdom: Cambridge University Press, 1990.
31. Lauffenburger, D. A., and Horwitz, A. F. Cell migration: a physically integrated molecular process. Cell, *84:* 359–369, 1996.
32. Van Aelst, L., and D'Souza-Schorey, C. Rho GTPases and signaling networks. Genes Dev., *11:* 2295–2322, 1997.
33. Maekawa, M., Ishizaki, T., Boku, S., Watanabe, N., Fujita, A., Iwamatsu, A., Obinata, T., Ohashi, K., Mizuno, K., and Narumiya, S. Signaling from Rho to the actin cytoskeleton through protein kinases ROCK and LIM-kinase. Science (Wash. DC), *285:* 895–898, 1999.
34. Post, P. L., Bokoch, G. M., and Mooseker, M. S. Human myosin-IXb is a mechanochemically active motor and a GAP for rho. J. Cell Sci., *111:* 941–950, 1998.
35. Matsuoka, Y., Li, X., and Bennett, V. Adducin is an in vivo substrate for protein kinase C: phosphorylation in the MARCKS-related domain inhibits activity in promoting spectrin-actin complexes and occurs in many cells, including dendritic spines of neurons. J. Cell Biol., *142:* 485–947, 1998.
36. Ruffner, D. E., Stormo, G. D., and Uhlenbeck, O. C. Sequence requirements of the hammerhead RNA self-cleavage reaction. Biochemistry, *29:* 10695–10702, 1990.
37. Zoumadakis, M., and Tabler, M. Comparative analysis of cleavage rates after systematic permutation of the NUX consensus target motif for hammerhead ribozymes. Nucleic Acids Res., *23:* 1192–1196, 1995.
38. Zuker, M. On finding all suboptimal foldings of an RNA molecule. Science (Wash. DC), *244:* 48–52, 1989.

Nucleic Acids Research, 2003, Vol. 31, No. 3 981–987
DOI: 10.1093/nar/gkg184

siRNAs generated by recombinant human Dicer induce specific and significant but target site-independent gene silencing in human cells

Hiroaki Kawasaki[1,2], Eigo Suyama[1,2], Mayu Iyo[1] and Kazunari Taira[1,2,*]

[1]Department of Chemistry and Biotechnology, School of Engineering, The University of Tokyo, Hongo, Bunkyo-ku, Tokyo 113-8656, Japan and [2]Gene Function Research Laboratory, National Institute of Advanced Industrial Science and Technology (AIST), Central 4, 1-1-1 Higashi, Tsukuba Science City 305-8562, Japan

Received October 7, 2002; Revised and Accepted November 19, 2002

ABSTRACT

RNA interference has emerged as a powerful tool for the silencing of gene expression in animals and plants. It was reported recently that 21 nt synthetic small interfering RNAs (siRNAs) specifically suppressed the expression of endogenous genes in several lines of mammalian cells. However, the efficacy of siRNAs is dependent on the presence of a specific target site within the target mRNA and it remains very difficult to predict the best or most effective target site. In this study, we demonstrate that siRNAs that have been generated *in vitro* by recombinant human Dicer (re-hDicer) significantly suppress not only the exogenous expression of a puromycin-resistance gene but also the endogenous expression of H-*ras*, c-*jun* and c-*fos*. In our system, selection of a target site is not necessary in the design of siRNAs. However, it is important to avoid homologous sequences within a target mRNA in a given protein family. Our diced siRNA system should be a powerful tool for the inactivation of genes in mammalian cells.

INTRODUCTION

RNA interference (RNAi) is a phenomenon whereby double-stranded RNA (dsRNA) induces the sequence-dependent degradation of a cognate mRNA in animal or plant cells (1–4). The mechanism responsible for dsRNA-induced gene silencing, which proceeds via a two-step mechanism, appears to have been strongly conserved during evolution (5–8). In the first step, long dsRNAs are recognized by a nuclease in the RNase III family known as Dicer, which cleaves the dsRNA into small interfering RNAs (siRNAs) (7) of 21–23 nt. These siRNAs are incorporated into a multicomponent nuclease complex, known as RISC, that is then responsible for the destruction of cognate mRNAs (9–11).

Since dsRNAs act as inactivating agents of specific genes, they have been utilized as tools for the functional analysis of genes in a nematode, the fruit fly and plants (12–14). It has been reported that, in mammalian cells, long dsRNAs induce the sequence-specific silencing of genes in mouse embryonal carcinoma cells and embryonic stem cells (15,16). However, long dsRNAs (of >30 nt in length) activate a dsRNA-dependent protein kinase (PKR) and 2′,5′-oligoadenylate synthetase (17) in mammalian somatic cells and the activities of these enzymes lead to a non-specific reduction in levels of mRNAs.

It was reported recently that synthetic 21 nt siRNAs specifically suppressed the expression of endogenous genes in several lines of mammalian cells (18). Use of these 21 nt siRNA duplexes circumvented the activation of PKR and 2′,5′-oligoadenylate synthetase and suggested that siRNAs might be useful as gene-inactivating agents in mammals. However, the efficacy of siRNAs is dependent on identification of a specific target site within a target mRNA (19). To obtain effective siRNAs, it is necessary, although both costly and time-consuming, to design and synthesize many different siRNAs.

In this report, we demonstrate that siRNAs generated *in vitro* by recombinant human Dicer (re-hDicer) significantly suppressed not only the exogenous expression of a puromycin-resistance gene but also the endogenous expression of H-*ras*, c-*jun* and c-*fos*. As reported recently, it is possible to produce short dsRNAs using RNase III from *Escherichia coli* (20). However, since dsRNAs of 12–15 nt in length, on average, are generated by this RNase III (21), it is better to use re-hDicer, which generates a more uniform population of 21–23 nt siRNAs. Use of re-hDicer to generate siRNAs might provide a powerful tool for studies of the mechanism of RNAi and the functions of various genes in mammalian cells, with potential utility in a clinical setting.

MATERIALS AND METHODS

Cloning of the human gene for Dicer and purification of re-hDicer

Partial cDNAs for human dicer/HERNA (nucleotides 379–1657 and 1390–7037) in the pBluescript vector (Stratagene, CA) were a gift from Dr S. Matsuda of the

*To whom correspondence should be addressed at Department of Chemistry and Biotechnology, School of Engineering, The University of Tokyo, Hongo, Tokyo 113-8656, Japan. Tel: +81 3 5841 8828; Fax: +81 298 61 3019; Email: taira@chembio.t.u-tokyo.ac.jp

University of Nagoya (22). We amplified the Dicer 5′ coding region (nucleotides 183–902) from a HeLa cDNA library by PCR with specific primers (forward primer, 5′-ATG AAA AGC CCT GCT TTG CAA CCC CT-3′; reverse primer, 5′-AGT TGC AGT TTC AGC ATT ACT CTT-3′) and then we cloned the amplified DNA into the TA cloning vector (Invitrogen, CA). Then we cloned the full-length human gene for Dicer from these partial cDNAs for human Dicer (hDicer). We digested full-length cDNA for hDicer and subcloned the blunt-ended fragment into the PinPoint™-Xa vector (Promega, Madison, WI), which contained the coding sequence for a biotin-binding region, using an *Eco*RV site. The hDicer expression plasmid was introduced into *E.coli* with 2 μM biotin and expressed upon induction with 100 μM IPTG. Then, cells were collected and pelleted by centrifugation at 5000 r.p.m. for 10 min. Cells were resuspended in lysis buffer [100 mM NaCl, 0.5 mM EDTA, 1% Triton X-100, 1 mM dithiothreitol, 2 mM phenylmethylsulfonyl fluoride, 50 mM Tris–HCl (pH 8.0)]. Then re-hDicer was purified on SoftLink™ resin (Promega) that included bound streptavidin, according to the manufacturer's protocol. For detection of re-hDicer, an aliquot of the resultant preparation of re-hDicer (0.5 μg) was fractionated by SDS–PAGE (10% polyacrylamide) and transferred to a PVDF membrane (Funakoshi Co., Tokyo, Japan) by electroblotting. Then re-hDicer was visualized with an ECL kit (Amersham Co., Little Chalfont, UK) and streptavidin-conjugated alkaline phosphatase.

Preparation of long dsRNAs and siRNAs

To generate the long dsRNA, a puromycin-resistance gene (nucleotides 1–300), the H-*ras* gene (nucleotides 370–570), the c-*jun* gene (nucleotides 1–200) and the c-*fos* gene (nucleotides 1–200) were amplified by PCR with a specific forward primer that contained a T7 promoter and a specific reverse primer that contained an SP6 promoter. Then, sense strand RNAs were generated by T7 RNA polymerase and antisense strand RNAs were generated by SP6 RNA polymerase. All siRNAs directed against puromycin-resistance mRNA and H-*ras* mRNA were synthesized by Japan Bio Service Co. Ltd (Saitama, Japan). Ten target sites (sites 1–10) were chosen for the synthetic siRNAs directed against the puromycin-resistance mRNA (site 1, 5′-ATG ACC GAG TAC AAG CCC A-3′; site 2, 5′-CTC GCC ACC CGC GAC GAC G-3′; site 3, 5′-CAC CGT CGA CCC GGA CCG C-3′; site 4, 5′-GAA CTC TTC CTC ACG CGC G-3′; site 5, 5′-GGT GTG GGT CGC GGA CGA C-3′; site 6, 5′-CAG ATG GAA GGC CTC CTG G-3′; site 7, 5′-GGA GCC CGC GTG GTT CCT G-3′; site 8, 5′-GGG TCT GGG CAG CGC CGT C-3′; site 9, 5′-CCT CCC CTT CTA CGA GCG G-3′; site 10, 5′-GCC CGG TGC CTG ACG CCC G-3′). Ten target sites (sites 1–10) were chosen for the synthetic siRNAs against H-*ras* mRNA (site 1, 5′-ATG ACG GAA TAT AAG CTT G-3′; site 2, 5′-GTT GGC GCC GGC GGT GTG G-3′; site 3, 5′-TAC GAC CCC ACT ATA GAG G-3′; site 4, 5′-AGG AGG AGT ACA GCG CCA T-3′; site 5, 5′-CAA CAC CAA GTC TTT TGA G-3′; site 6, 5′-GGA CTC GGA TGA CGT GCC C-3′; site 7, 5′-TCT CGG CAG GCT CAG GAC C-3′; site 8, 5′-GAC CCG GCA GGG AGT GGA G-3′; site 9, 5′-GCT GCGGAA GCT GAA CCC T-3′; site 10, 5′-GTG TGT GCT CTC CTG AGG A-3′). Then, to generate siRNAs, all RNAs were annealed by the standard method (6).

Processing *in vitro* by re-hDicer and purification of diced siRNAs

To examine the activity of hDicer, we mixed 10 μg of dsRNA with 1 μg of re-hDicer in 200 μl of reaction buffer [100 mM NaCl, 20 mM HEPES, 1 mM ATP, 5 mM $MgCl_2$, 50 mM Tris–HCl (pH 7.0)]. The mixture was incubated for 30 min at 37°C. Then, 20 μl of the reaction mixture were fractionated by electrophoresis on a non-denaturing 12% polyacrylamide gel. Bands of RNA were detected with Syber™ green II reagent (Nippon Gene, Toyama, Japan). We recovered siRNAs of 21–23 nt in length from the reaction mixture using a QIAquick™ nucleotide-removal kit (Qiagen, Hilden, Germany). The siRNAs were precipitated in ethanol and then dissolved in TE buffer. The concentration of diced siRNAs was determined by monitoring absorbance at 260 nm.

Transfection of cells and assay of cell viability

HeLa cells were cultured in DMEM supplemented with 10% fetal bovine serum. Transfections with either 20 nM siRNAs or diced siRNAs were performed using the Oligofectamine™ reagent (Invitrogen) in accordance with the manufacturer's instructions. Cell viability was determined with trypan blue as described.

Western blotting

HeLa cells that had been transfected with individual siRNAs were harvested. Proteins were resolved by SDS–PAGE (10% polyacrylamide) and transferred to a PVDF membrane (Funakoshi Co.) by electroblotting. Immune complexes were visualized with an ECL™ kit, using specific polyclonal antibodies against H-Ras (Oncogene Research Products, San Diego, CA), N-Ras (Oncogene Research Products), K-Ras (Oncogene Research Procducts), c-Jun (Santa Cruz Biotechnology, Santa Cruz, CA), c-Fos (Santa Cruz Biotechnology) and actin (Oncogene Research Products), as an endogenous control. Quantitation was performed by densitometry and NIH Image Analysis.

RESULTS

Cloning of a human gene for Dicer and purification and characterization of re-hDicer

To prepare heterogeneous siRNAs that could target various sites in a specific target mRNA, we used hDicer, which participates in RNAi in human cells. Initially, to generate re-hDicer using a bacterial expression system, we cloned the full-length human gene for Dicer using partial cDNAs for hDicer (see Materials and Methods; 7,22). The full-length cDNA was then subcloned into the PinPoint™-Xa vector that contained the coding region for the biotin-binding region of a biotin ligase for subsequence purification of the recombinant protein.

We introduced the hDicer expression plasmid (phDicer) into *E.coli* and, with biotin in the culture medium, re-hDicer was expressed upon induction with IPTG. The re-hDicer with bound biotin was purified by a 'pull-down' method with beads to which streptavidin had been bound (see Materials and Methods) and analyzed by SDS–PAGE, after which re-hDicer was detected by western blotting with visualization using alkaline phosphatase-conjugated streptavidin. As shown in

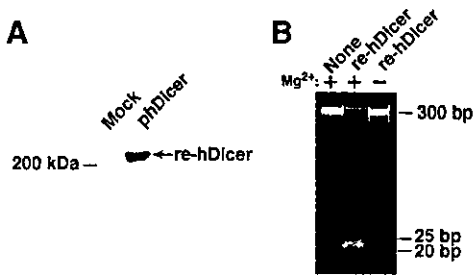

Figure 1. (A) Detection of the hDicer-mediated generation of diced siRNAs. Re-hDicer was synthesized in *E.coli* and detected by western blotting analysis, as described in the text. The preparation of re-hDicer (0.5 μg) was fractionated by SDS–PAGE (10% polyacrylamide) and transferred to a PVDF membrane by electroblotting. Then re-hDicer was visualized with an ECL kit and streptavidin-conjugated alkaline phosphatase. Mock, preparation from cells transfected with the empty plasmid; phDicer, preparation from cells infected with an expression plasmid that encoded hDicer. (B) Generation of siRNAs by re-hDicer. Long dsRNA (10 μg) was mixed with 1 μg of re-hDicer in 200 μl of reaction buffer, with or without 5 mM $MgCl_2$. The reaction mixtures were incubated for 30 min at 37°C. Then 20 μl of each reaction mixture were fractionated by electrophoresis in a 12% non-denaturing polyacrylamide gel. siRNAs of 20–25 nt in length were detected with Syber™ green II.

Figure 1A, we detected re-hDicer with a biotin tag by western blotting. The putative molecular mass of the biotin-labeled re-hDicer was ~220 kDa. Mock transfection with a vector that did not include the cDNA for hDicer did not yield the corresponding protein, confirming the production of re-hDicer in this expression system in *E.coli*.

Next, to determine whether the re-hDicer had RNase III activity, we performed a processing assay *in vitro* using long dsRNAs that had been generated by transcription *in vitro*. To construct long dsRNAs for use as substrates, we amplified a puromycin-resistance gene (nucleotides 1–300) by PCR using a specific forward primer that contained a T7 promoter and a specific reverse primer that contained an SP6 promoter. Then sense strand RNAs were generated by T7 RNA polymerase and antisense strand RNAs were generated by an SP6 RNA polymerase. These transcribed RNAs were annealed by the standard method (6). Then, the long dsRNAs and re-hDicer were combined and incubated in an appropriate reaction mixture (see Materials and Methods) for 30 min at 37°C. As shown in Figure 1B, siRNAs of 20–25 nt in length were generated in the presence of re-hDicer. In contrast, in the absence of either re-hDicer or Mg^{2+} ions, no such siRNAs were detected (lanes 1 and 3). Thus, re-hDicer exhibited Mg^{2+}-dependent dsRNA processing activity. It was reported recently that recombinant hDicer in insect cells also exhibits RNase III activity (23,24).

Effects of diced siRNAs on expression of an exogenous puromycin-resistance gene

In mammalian cells, synthetic 21 nt siRNAs suppress the expression of both reporter genes and endogenous genes to a significant extent (18,19,25). While long dsRNAs (>30 nt) activate PKR and 2′,5′-oligoadenylate synthetase, use of these shorter siRNAs circumvents the activation of these enzymes and activates the RNAi pathway. Thus, these siRNAs might be expected to be useful for the sequence-specific silencing of gene expression. However, the dependence of the activity of siRNAs on the target site has been reported (19), and it remains very difficult to predict the best and most effective target site. Since the dependence of the activity of siRNAs on the target site was examined only in the case of the human gene for tissue factor (19), we further investigated the dependence on target site using siRNAs targeted to a puromycin-resistance gene and directed against 10 target sites within this gene (Fig. 2A and B). We used siRNA targeted to GL3-luciferase as a control.

To prepare diced siRNAs, we transcribed both sense and antisense strands of a partial mRNA for puromycin resistance (nucleotides 1–300) *in vitro*, using T7 and SP6 RNA polymerases (Fig. 1B). After the dicing of dsRNAs *in vitro*, we purified the diced siRNAs using a QIAquick™ nucleotide-removal kit. Next, we introduced each siRNA (20 nM) and the expression plasmid for a puromycin-resistance gene into HeLa cells using the Oligofectamine™ reagent. After 36 h, we treated the HeLa cells with puromycin and determined cell viability using trypan blue. The efficiency of transfection of each siRNA was measured with the luciferase gene from *Renilla* as a reporter gene.

As shown in Figure 2C, in the presence of siRNA targeted to GL3-luciferase, cell viability remained the same as that of wild-type HeLa cells. The viability of cells that had been treated with site 2-, site 3-, site 4-, site 5- and site 10-specific siRNAs was significantly lower than that of wild-type cells that harbored the puromycin-resistance gene. In contrast, site 1-, site 6-, site 7-, site 8- and site 9-specific siRNAs had lower growth-inhibitory activity. These results indicated that the efficiency of siRNAs that were specific for the puromycin-resistance gene depended on the target site within the target mRNA.

As we had anticipated, diced siRNAs that corresponded to unlimited target sites within the specific mRNA were more effective than any specific siRNA or a mixture of site 1-, site 2-, site 3-, site 4- and site 5-specific siRNAs. When we analyzed the GC content of target sites and the secondary structure of the target gene, as predicted with the mfold program (Fig. 2B) (26), we failed to recognize a clear correlation between either secondary structure or GC content (Table 1) and effective and less effective target sites. In the case of the target gene, siRNAs targeted to regions from position 20 to position 280 and near the 3′ end of the target gene were more effective than others that we tested.

Effects of diced siRNAs on expression of an endogenous H-*ras* gene

To examine the effects of diced siRNAs on expression of an endogenous gene, we selected the H-*ras* gene as a target. The H-*ras* gene is a member of the *ras* family, which also includes K-*ras* and N-*ras* (27). Again, to check the dependence on target site of the effects of siRNAs, we selected 10 target sites in the H-*ras* gene (Fig. 3A and B). For construction of diced siRNAs, we searched for a region of low homology to other members of the *ras* family in the H-*ras* gene. We selected such a region of the H-*ras* gene (nucleotides 370–570) as the long dsRNA substrate. Diced siRNAs targeted to the H-*ras* gene were generated by the same method as described above. Each individual siRNA (20 nM) was introduced into HeLa cells using the Oligofectamine™ reagent. After 72 h, cells were

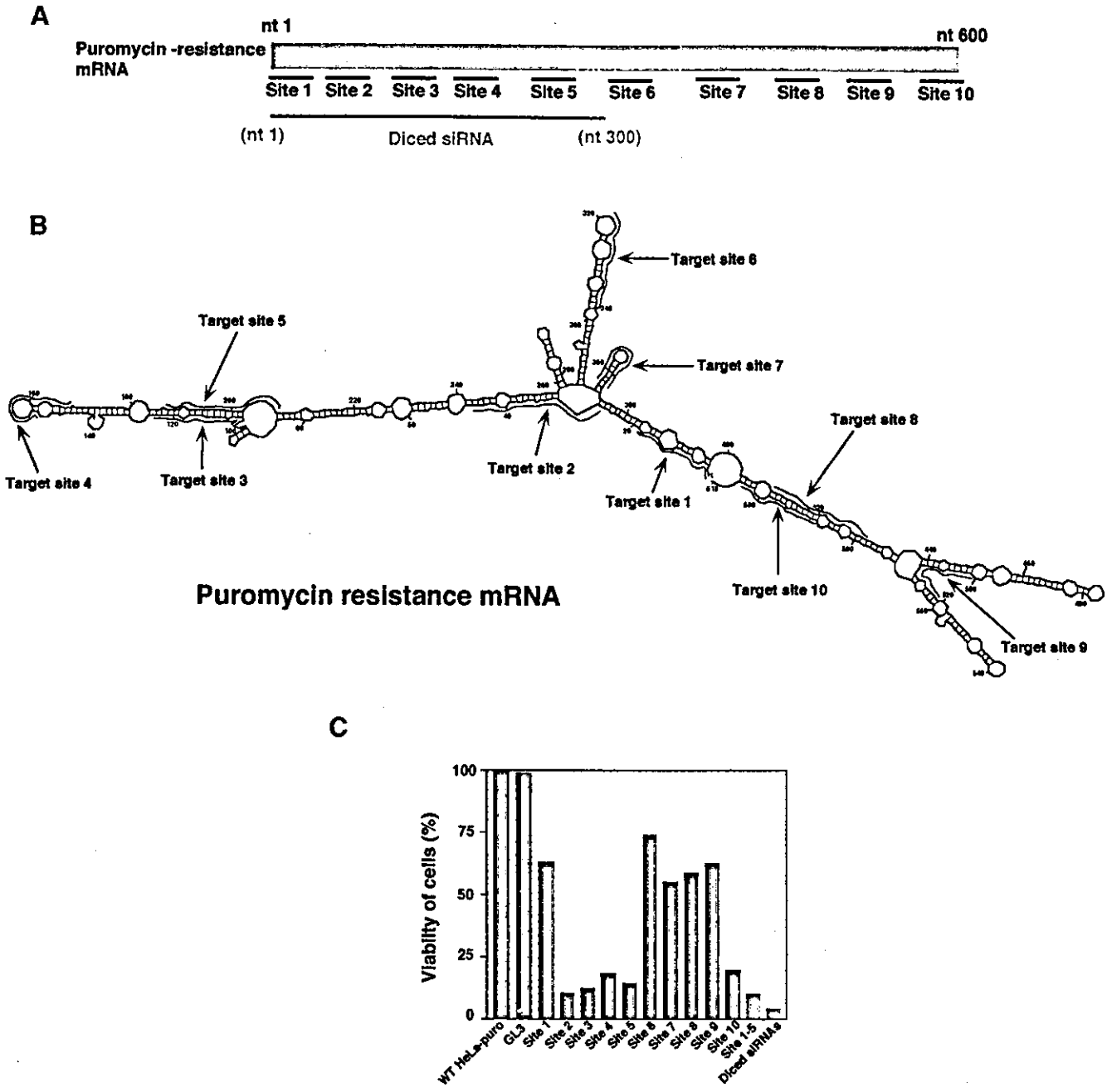

Figure 2. Suppression of the expression of an exogenous puromycin-resistance gene. (**A**) Ten sites (sites 1–10) were chosen as targets for synthetic siRNAs, as detailed in the text. For preparation of diced siRNAs, long dsRNAs corresponding to the 5′ region of the puromycin-resistance gene (nucleotides 1–300) were generated and treated with re-hDicer. (**B**) The secondary structure of the puromycin-resistance mRNA as predicted by the mfold program (24). (**C**) Diced siRNAs were the most effective suppressors of the expression of the exogenous puromycin-resistance gene (as indicated by the bar on the far right of the histogram). The efficiency of transfections with siRNAs was monitored with a reporter gene for luciferase from *Renilla*.

collected and total proteins were extracted. Levels of H-Ras protein were monitored by western blotting with specific antibodies. We determined levels of actin similarly as an endogenous control. Quantitation of proteins was performed by densitometry and NIH Image Analysis.

As shown in Figure 3C, the levels of H-Ras in cells that had been treated with site 2-, site 3-, site 4-, site 5- and site 9-specific siRNAs were significantly lower than that in wild-type HeLa cells. In contrast, site 1-, site 6-, site 7- and site 8-specific siRNAs had lower inhibitory activity. We normalized the results by reference to levels of actin and the results indicated that the efficiency of the siRNAs depended on the target site in the endogenous H-*ras* gene. In the case of both the puromycin-resistance gene and the H-*ras* gene, synthetic siRNAs targeted to the central regions of the genes were less effective. As for the diced siRNAs, they were

Table 1. GC contents (%) of the target site of each siRNA and levels of inhibition of gene expression

Target site	Puromycin-resistance mRNA		H-*ras* mRNA	
	GC (%)	Inhibition (%)	GC (%)	Inhibition (%)
1	52.6	37.2	36.0	63.2
2	78.9	88.6	78.9	81.7
3	78.9	86.9	52.6	78.6
4	63.1	79.5	57.8	87.8
5	73.6	84.6	42.0	70.5
6	73.6	24.8	68.4	45.3
7	73.6	45.1	68.4	23.6
8	78.9	40.5	73.6	36.8
9	68.4	36.8	63.1	74.2
10	84.0	78.2	57.8	82.1

significantly more effective than all the other siRNAs tested and than a mixture of siRNAs (site 7-, site 8-, site 9- and site 10-specific siRNAs) targeted to the H-*ras* gene. The levels of K-Ras and N-Ras proteins in cells that had been treated with diced siRNAs were, as anticipated, similar to those in wild-type HeLa cells (Fig. 3D). Thus, the diced siRNAs did not affect the expression of either the K-*ras* or the N-*ras* gene.

A structural analysis (Fig. 3B) similar to that shown in Figure 2B again failed to indicate any correlation between GC content (Table 1) and the extent of inhibition by siRNAs. Since results obtained in a previous study suggested that the effects of siRNAs, oligonucleotides and ribozymes might share some common features (28), it seems likely that more experimental data related to the accessibility of target mRNAs *in vitro* and *in vivo* (rather than computer-predicted secondary structures, as shown, for example, in Fig. 3B) are needed for a more precise examination of such putative relationships. In the case of H-*ras*, again, siRNAs targeted to certain regions (from position 20 to 280 and near the 3′ end) in the target gene were more effective than others, and diced siRNAs were again much more effective than individual siRNAs or a mixture of such siRNAs (Fig. 3C). These results resembled those obtained with the puromycin-resistance gene. It is possible that the higher activity of the diced siRNAs than that of individual siRNAs might simply have been due to an additive effect of targeting multiple sites along a message. However, the results obtained with the mixture of siRNAs (site 7-, site 8-, site 9- and site 10-specific siRNAs) failed to support this interpretation. It is more likely that the effects of siRNAs are changed by even a small change in the target site (of even just a few nucleotides) and, thus, diced siRNAs appeared to include some populations that were significantly more effective than the combined individual siRNAs. The observations suggest the clear advantages of diced siRNAs over individual synthetic siRNAs, at least in the experiments carried out in this study.

Diced siRNAs directed against c-*jun* and c-*fos* mRNAs

Finally, to confirm the effects of diced siRNA, we generated diced siRNAs against c-*jun* mRNA and c-*fos* mRNA, respectively. We introduced these diced siRNAs into HeLa cells and, 72 h later, we collected the cells and extracted the total proteins. The levels of the c-Jun and c-Fos proteins were examined by western blotting with specific antibodies. As shown in Figure 4, the level of c-Jun in cells that had been transfected with diced siRNAs was significantly lower than that in wild-type HeLa cells. The levels of actin were similar in both transfected and wild-type cells. We obtained analogous results using diced siRNAs directed against c-*fos* mRNA. Our results confirmed the high potential utility of diced siRNAs in the silencing of specific genes in human cells.

DISCUSSION

In this study, we developed an effective gene-silencing method, which we refer to as diced siRNA technology, using re-hDicer. RNAi has been shown to be a powerful tool for studies of gene function in a nematode, the fruit fly and plants (12–14). Effective sequence-specific gene silencing in several animals requires dsRNA of >150 bp (8,9,29,30). However, in mammals, long dsRNAs (>30 nt) induce the non-specific reduction of gene expression via the activation of PKR. Synthetic siRNAs that can effectively suppress the expression of endogenous genes have been reported by several groups (18,19,25). However, the efficiency of siRNAs depends on a specific target site within the target gene (Figs 2 and 3).

In RNAi, siRNAs become associated with RISC and function as guide RNAs in the search for target sites (3). However, we do not yet know how the siRNA–RISC complex can gain access to its target site and how cleavage at the target site occurs. In the nematode *Caenorhabditis elegans*, a RNA-directed RNA polymerase (RdRP) chain reaction with siRNA amplifies the interference that is caused by a small amount of 'trigger' dsRNA (31). Thus, siRNA acts not only as a guide but also as a primer and long dsRNAs are generated by RdRP. These long dsRNAs are then cleaved into fragments of ~21 nt in length by Dicer.

Since accessibility of the siRNA might depend on the secondary structure of the target mRNA, we have to design and synthesize many different siRNAs to obtain effective siRNAs, and, at present, success depends on trial and error. To overcome these problems, we utilized re-hDicer for dicing of long dsRNAs *in vitro* and no longer needed to select a target site. However, it remained important to avoid the selection of sequences homologous to those of other members of the family to which the target protein belonged. Using our method, we succeeded in suppressing the expression of several

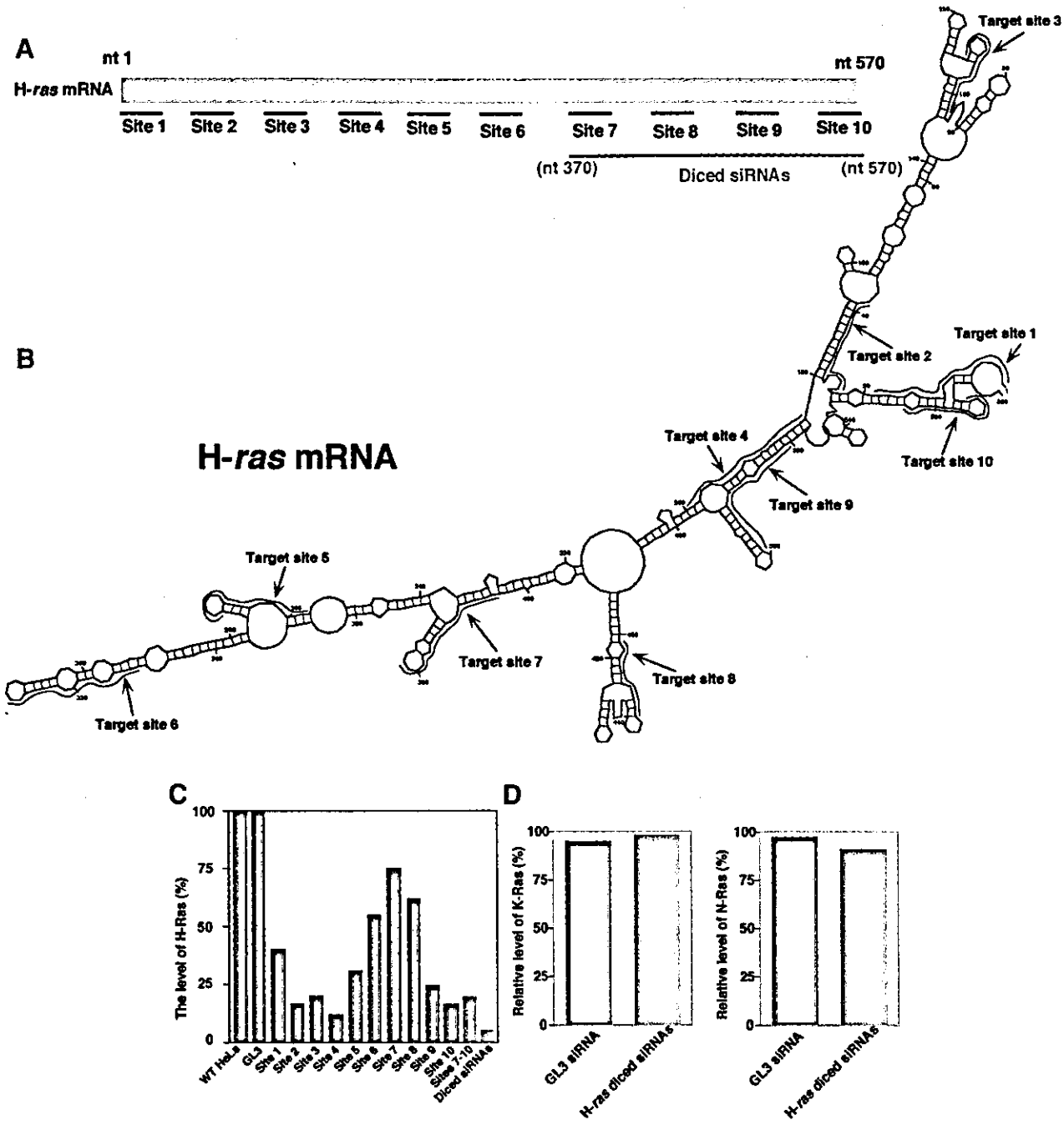

Figure 3. Suppression of the expression of the endogenous H-*ras* gene. (**A**) Ten sites (sites 1–10) were chosen as targets for synthetic siRNAs, as detailed in the text. For the preparation of diced siRNAs, long dsRNAs corresponding to the 3′ region of the H-*ras* gene (nucleotides 370–570), which exhibited weak homology to the sequences of related *ras* genes, were generated and treated with re-hDicer. (**B**) The secondary structure of H-*ras* mRNA, as predicted by the mfold program (24). (**C**) Diced siRNAs were the most effective suppressors of the expression of the endogenous H-*ras* gene (as indicated by a bar on the far right of the histogram). The results were normalized by reference to levels of actin, as a control. (**D**) Effects of diced siRNAs targeted to the H-*ras* gene on the expression of the related K-*ras* and N-*ras* genes. K-Ras and N-Ras were detected by western blotting analysis with specific antibodies. Levels were quantitated by densitometry and NIH Image Analysis.

endogenous genes that included H-*ras*, c-*jun* and c-*fos*, as shown in Figures 3 and 4. It appears, therefore, that the diced siRNA technology might be a powerful tool for the functional analysis of genes of interest, as well as for inactivation of specific genes in a clinical setting.

ACKNOWLEDGEMENTS

The authors thank Dr S. Matsuda of Nagoya University for gifts of partial cDNAs for hDicer and Dr Laura Nelson of AIST for critical reading of and helpful comments on the

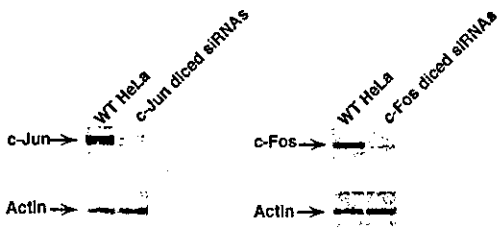

Figure 4. Suppression of the expression of the endogenous c-*jun* and c-*fos* genes by diced siRNAs. For the preparation of diced siRNAs, long dsRNAs corresponding to the 5′ region of the c-*jun* gene (nucleotides 1–200) and the c-*fos* gene (nucleotides 1–200) were generated and treated with re-hDicer. Both c-Jun and c-Fos were detected by western blotting analysis with specific antibodies. Actin was used as an endogenous control. WT-HeLa, wild-type HeLa cells; c-Jun (c-Fos) diced siRNs, siRNAs generated from c-*jun*-specific (c-*fos*-specific) dsRNA.

original manuscript. This research was supported by grants from the Ministry of Economy, Trade and Industry (METI) of Japan and by a Grant-in-Aid for Scientific Research from the Ministry of Education, Culture, Sports, Science and Culture (MEXT) of Japan.

REFERENCES

1. Fire,A., Xu,S., Montgomery,M.K., Kostas,S.A., Driver,S.E. and Mello,C.C. (1998) Potent and specific genetic interference by double-stranded RNA in *Caenorhabditis elegans*. *Nature*, **391**, 806–811.
2. Sharp,P.A. (2001) RNA interference-2001. *Genes Dev.*, **15**, 485–490.
3. Hutvagner,G. and Zamore,P.D. (2002) RNAi: nature abhors a double-strand. *Curr. Opin. Genet. Dev.*, **12**, 225–232.
4. Hannon,G.J. (2002) RNA interference. *Nature*, **418**, 244–251.
5. Zamore,P., Tuschl,T., Sharp,P. and Bartel,D. (2000) RNAi: double-stranded RNA directs the ATP-dependent cleavage of mRNA at 21- to 23-nucleotide intervals. *Cell*, **101**, 25–33.
6. Elbashir,S.M., Lendeckel,W. and Tuschl,T. (2001) RNA interference is mediated by 21- and 22-nucleotide RNAs. *Genes Dev.*, **15**, 188–200.
7. Bernstein,E., Caudy,A.A., Hammond,S.M. and Hannon,G.J. (2001) Role for a bidentate ribonuclease in the initiation step of RNA interference. *Nature*, **409**, 363–366.
8. Tuschl,T., Zamore,P.D., Lehmann,R., Bartel,D.P. and Sharp,P.A. (1999) Targeted mRNA degradation by double-stranded RNA *in vitro*. *Genes Dev.*, **13**, 3191–3197.
9. Hammond,S.M., Bernstein,E., Beach,D. and Hannon,G.J. (2000) An RNA-directed nuclease mediates post-transcriptional gene silencing in *Drosophila* cells. *Nature*, **404**, 293–296.
10. Hammond,S.M., Boettcher,S., Caudy,A.A., Kobayashi,R. and Hannon,G.J. (2001) Argonaute 2, a link between genetic and biochemical analysis of RNAi. *Science*, **293**, 1146–1150.
11. Bernstein,E., Denli,A.M. and Hannon,G.J. (2001) The rest is silence. *RNA*, **7**, 1509–1521.
12. Vaucheret,H., Beclin,C. and Fagard,M. (2001) Post-transcriptional gene silencing in plants. *J. Cell Sci.*, **114**, 3083–3091.
13. Hammond,S.M., Caudy,A.A. and Hannon,G.J. (2001) Post-transcriptional gene silencing by double-stranded RNA. *Nature Rev. Genet.*, **2**, 110–119.
14. Grishok,A. and Mello,C.C. (2002) RNAi (nematodes: *Caenorhabditis elegans*). *Adv. Genet.*, **46**, 339–360.
15. Billy,E., Brondani,V., Zhang,H., Müller,U. and Filipowicz,W. (2001) Specific interference with gene expression induced by long, double-stranded RNA in mouse embryonal teratocarcinoma cell lines. *Proc. Natl Acad. Sci. USA*, **98**, 14428–14433.
16. Paddison,P.J., Caudy,A.A. and Hannon,G.J. (2002) Stable suppression of gene expression by RNAi in mammalian cells. *Proc. Natl Acad. Sci. USA*, **99**, 1443–1448.
17. Stark,G.R., Kerr,I.M., Williams,B.R., Silverman,R.H. and Schreiber,R.D. (1998) How cells respond to interferons. *Annu. Rev. Biochem.*, **67**, 227–264.
18. Elbashir,S.M., Harborth,J., Lendeckel,W., Yalcin,A., Weber,K. and Tuschl,T. (2001) Duplexes of 21-nucleotide RNAs mediate RNA interference in mammalian cell culture. *Nature*, **411**, 494–498.
19. Holen,T., Amarzguioui,M., Wiiger,M.T., Babaie,E. and Prydz,H. (2002) Positional effects of short interfering RNAs targeting the human coagulation trigger Tissue Factor. *Nucleic Acids Res.*, **30**, 1757–1766.
20. Yang,D., Buchholz,F., Huang,Z., Goga,A., Chen,C.Y., Brodsky,F.M. and Bishop,J.M. (2002) Short RNA duplexes produced by hydrolysis with *Escherichia coli* RNase III mediate effective RNA interference in mammalian cells. *Proc. Natl Acad. Sci. USA*, **99**, 9942–9947.
21. Amarasinghe,A.K., Calin-Jageman,I., Harmouch,A., Sun,W. and Nicholson,A.W. (2001) *Escherichia coli* ribonuclease III: affinity purification of hexahistidine-tagged enzyme and assays for substrate binding and cleavage. *Methods Enzymol.*, **342**, 143–158.
22. Matsuda,S., Ichigotani,Y., Okuda,T., Irimura,T., Nakatsugawa,S. and Hamaguchi,M. (2000) Molecular cloning and characterization of a novel human gene (*HERNA*) which encodes a putative RNA-helicase. *Biochim. Biophys. Acta*, **1490**, 163–169.
23. Harborth,J., Elbashir,S.M., Bechert,K., Tuschl,T. and Weber,K. (2001) Identification of essential genes in cultured mammalian cells using small interfering RNAs. *J. Cell Sci.*, **114**, 4557–4565.
24. Provost,P., Dishart,D., Doucet,J., Frendewey,D., Samuelsson,B. and Radmark,O. (2002) Ribonuclease activity and RNA binding of recombinant human Dicer. *EMBO J.*, **21**, 5864–5874.
25. Zhang,H., Kolb,F.A., Brondani,V., Billy,E. and Filipowicz,W. (2002) Human Dicer preferentially cleaves dsRNAs at their termini without a requirement for ATP. *EMBO J.*, **21**, 5875–5885.
26. Zuker,M., Mathews,D.H. and Turner,D.H. (1999) Algorithms and thermodynamics for RNA secondary structure prediction: a practical guide. In Barciszewski,J. and Clark,B.F.C. (eds), *RNA Biochemistry and Biotechnology*. Kluwer Academic, Hingham, MA.
27. Adjei,A.A. (2001) Blocking oncogenic Ras signaling for cancer therapy. *J. Natl Cancer Inst.*, **93**, 1062–1074.
28. Miyagishi,M., Hayashi,M. and Taira,K. (2003) Comparison of the suppressive effects of antisense oligonucleotides and siRNAs directed against the same targets in mammalian cells. *Antisense Nucleic Acid Drug Dev.*, in press.
29. Caplen,N.J., Fleenor,J., Fire,A. and Morgan,R.A. (2000) dsRNA-mediated gene silencing in cultured *Drosophila* cells: a tissue culture model for the analysis of RNA interference. *Gene*, **252**, 95–105.
30. Ngo,H., Tschudi,C., Gull,K. and Ullu,E. (1998) Double-stranded RNA induces mRNA degradation in *Trypanosoma brucei*. *Proc. Natl Acad. Sci. USA*, **95**, 14687–14692.
31. Sijen,T., Fleenor,J., Simmer,F., Thijssen,K.L., Parrish,S., Timmons,L., Plasterk,R.H. and Fire,A. (2001) On the role of RNA amplification in dsRNA-triggered gene silencing. *Cell*, **107**, 465–476.

EMBO
reports

scientific report

Targeting mortalin using conventional and RNA-helicase-coupled hammerhead ribozymes

Renu Wadhwa[1,3], *Hiroshi Ando*[3], *Hiroaki Kawasaki*[4], *Kazunari Taira*[1,4] & *Sunil C. Kaul*[2]*

[1]Gene Function Research Center and [2]Research Center for Glycoscience, National Institute of Advanced Industrial Science and Technology, Higashi, Tsukuba, Ibaraki, Japan, [3]Chugai Research Institute for Medical Sciences, Nagai, Niihari-mura, Ibaraki, Japan, and [4]Department of Chemistry and Biotechnology, Graduate School of Engineering, The University of Tokyo, Hongo, Tokyo, Japan

Mortalin, also known as mot2/mthsp70/GRP75/PBP74, is a member of the heat-shock protein 70 family that is heat-uninducible. It is differentially distributed in cells that have normal and immortal phenotypes, has been localized to various subcellular sites, and has several binding partners and functions. Here, we describe the construction and use of mortalin-specific conventional and hybrid ribozymes to elucidate its crucial role in cell proliferation. Whereas conventional hammerhead ribozymes did not cause any repression of endogenous mortalin expression, RNA-helicase-linked hybrid ribozymes successfully suppressed the expression of mortalin, which resulted in the growth arrest of transformed human cells. We show that, first, RNA helicase-coupled hybrid ribozymes that have a linked unwinding activity can be used to target genes for which conventional hammerhead ribozymes are ineffective; second, the targeting of mortalin by RNA-helicase-coupled hybrid ribozymes causes growth suppression of transformed human cells and could be used as a treatment for cancer.

EMBO reports 4, 595–601 (2003)
doi:10.1038/sj.embor.embor855

INTRODUCTION

Ribozymes are RNA molecules that have enzymatic properties (Cech, 1986). They are naturally occurring molecules that provide fine-tuning of gene expression cascades (replication, transcription and translation) by catalysing essential steps such as cleavage and ligation (Zhang & Cech, 1997; Cech, 2000; Doudna & Cech, 2002). Hammerhead ribozymes are the smallest ribozymes, and are used as 'molecular scissors' in molecular biology and biotechnology to elucidate and eliminate gene functions. The ribozyme RNA is induced to fold into its active conformation by the binding of metal ions. It forms two domains: the scaffold (domain 2) on which the ribozyme is built, and the active centre (the catalytic domain; known as domain 1; Cech & Uhlenbeck, 1994; Hammann & Lilley, 2002). During the past two decades, the mechanism of action of hammerhead ribozymes, describing the requirement for divalent metal ions, definition of the catalytic domains, and the sequence specificity, which is usually referred to as the target site, has been shown (Kawasaki *et al.*, 1996; Koseki *et al.*, 1999; Takagi *et al.*, 2001; Kato *et al.*, 2001; Akashi *et al.*, 2002; Hammann & Lilley, 2002; Pyle, 2002). The activity of ribozymes *in vivo* is dependent on the level of expression at which they are effective, their specificity, and their intracellular stability, target colocalization and the accessibility of target sites (Yarus, 1999). These technical issues have caused severe problems for the use of ribozymes *in vivo*. Various modifications of the ribozyme expression plasmid have therefore come into play. For example, it has been shown that ribozymes expressed under the control of the RNA polymerase III promoter (the transfer RNA $(tRNA)^{Val}$ promoter) are efficiently expressed, highly stable and are exported to the cytoplasm (Kuwabara *et al.*, 2001; Miyagishi *et al.*, 2001). Such expression increased ribozyme activity *in vivo* many times over. However, ribozymes that are efficiently expressed and highly stable could still lack actvity because of inaccessibility of the target sites, which is a major problem because of unforeseeable secondary and tertiary RNA structures. Recently, this obstacle was elegantly resolved by modifying ribozyme expression plasmids. A new hybrid ribozyme that combined the cleavage activity of hammerhead ribozymes with the unwinding activity of endogenous RNA helicases was developed. Such RNA-helicase-based hybrid ribozymes, expressed from the RNA polymerase III promoter ($tRNA^{Val}$) were indeed shown to have substrate-unwinding activity, as well as a strong cleavage activity (Warashina *et al.*, 2001; Kawasaki & Taira, 2002; Kuwabara *et al.*, 2002).

Here, we show the use of conventional and RNA-helicase-linked hammerhead ribozymes to suppress mortalin expression. Mortalin (mot2/mthsp70/GRP75/PBP74) is a member of the heat-shock protein 70 family and is involved in pathways that regulate

[1]Gene Function Research Center and [2]Research Center for Glycoscience, National Institute of Advanced Industrial Science and Technology, 1-1-1 Higashi, Tsukuba, Ibaraki 305-8566, Japan
[3]Chugai Research Institute for Medical Sciences. 153-2 Nagai, Niihari-mura, Ibaraki 300-4101, Japan
[4]Department of Chemistry and Biotechnology Graduate School of Engineering, The University of Tokyo, Hongo, Tokyo 113-8656, Japan
*Corresponding author. Tel: +81 298 61 6713; Fax: +81 298 61 6052; E-mail: s-kaul@aist.go.jp

Received 20 December 2002; revised 7 April 2003; accepted 15 April 2003
Published online 23 May 2003

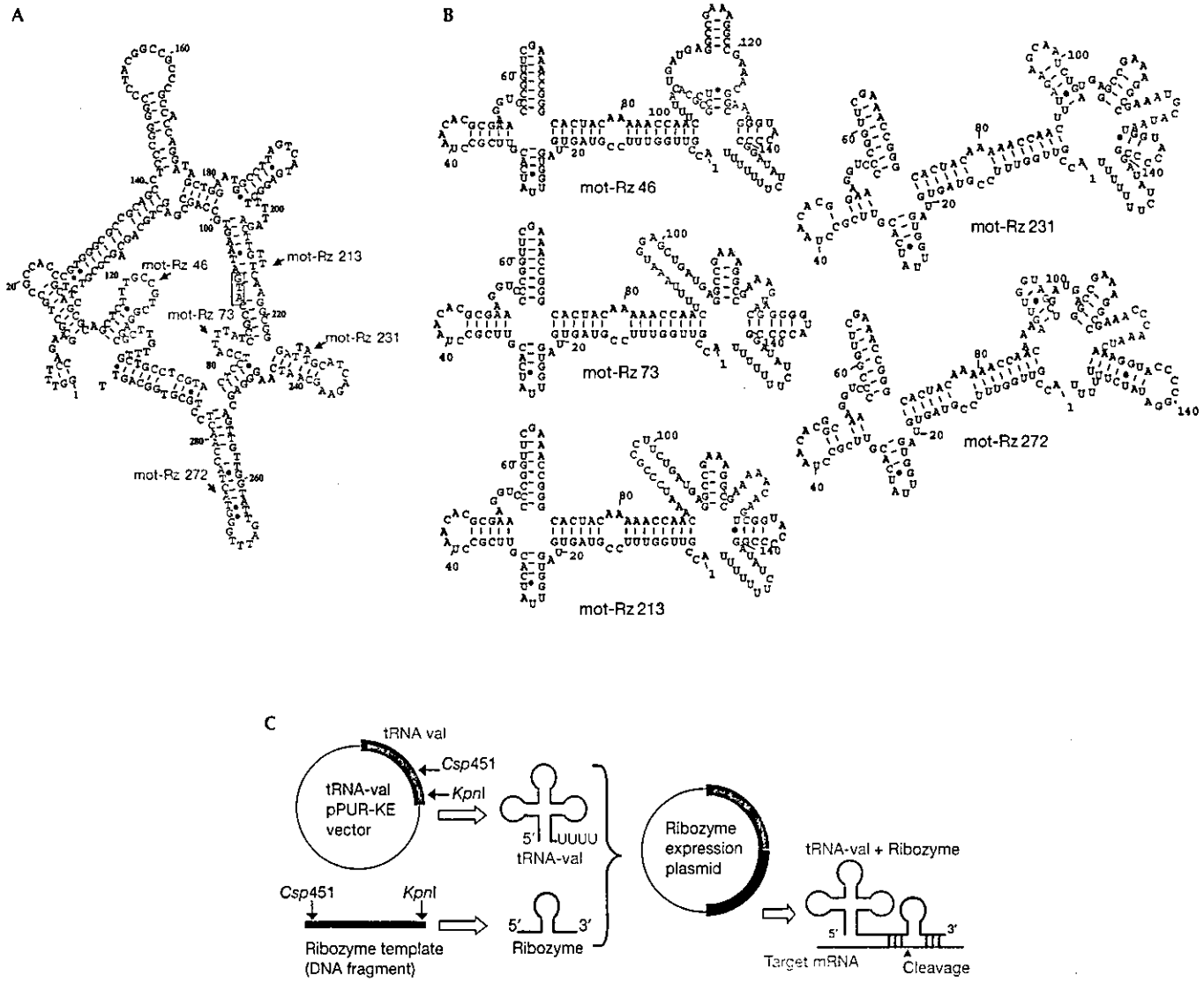

Fig. 1 | Design of mortalin ribozymes. (A) Partial secondary structure of mortalin RNA. Mortalin ribozyme (mot-Rz) target sites and cleavage sites are marked in red and green, respectively. The first ATG is shown in the blue box. (B) Partial secondary structures of each of the target sites, with the ribozyme and transfer RNA sequences (155 nucleotides) as predicted using the Mfold programme (Zuker, 1989). Target sites are marked in red. (C) Schematic representation of the construction and action of a hammerhead-ribozyme expression plasmid driven by a tRNA promoter. mRNA, messenger RNA.

cell proliferation, tumorigenesis and the stress response (Wadhwa *et al.*, 1993, 1998, 2002a,b). We report that whereas conventional hammerhead ribozymes were ineffective for all of the chosen target sites, some of the RNA-helicase-linked hybrid ribozymes successfully repressed mortalin expression, resulting in the growth arrest of transformed human cells.

RESULTS AND DISCUSSION

Conventional hammerhead ribozymes for mortalin

Five mortalin-specific ribozyme (mot-Rz) expression plasmids, which were driven by the $tRNA^{Val}$ promoter and which targeted its five different sites, were made as described in the Methods section, and are shown schematically in Fig. 1. We first examined the catalytic activity of these ribozymes for a mortalin–luciferase reporter-construct that encodes the amino-terminal region of mortalin in-frame with the luciferase reporter protein (as described in the Methods section, and in Fig. 2). COS7 cells were used for their high transfection efficiency. These cells were transfected with the mortalin reporter plasmid and the mot-Rz plasmids, as shown in Fig. 2B. Cells were lysed and assayed for luciferase activity 48 h after transfection. Cells transfected with mot-Rz plasmids showed a significant decrease (60–80%) in the mortalin–luciferase reporter activity as compared with the activity in the vector-only-transfected cells. This was interpreted as being a result of the cleavage of the mortalin–luciferase transcript by the mot-Rzs, suggesting that the mot-Rzs directed to these target sites might be effective *in vivo* to suppress the expression of endogenous mortalin. A second, more direct assay, in which mortalin

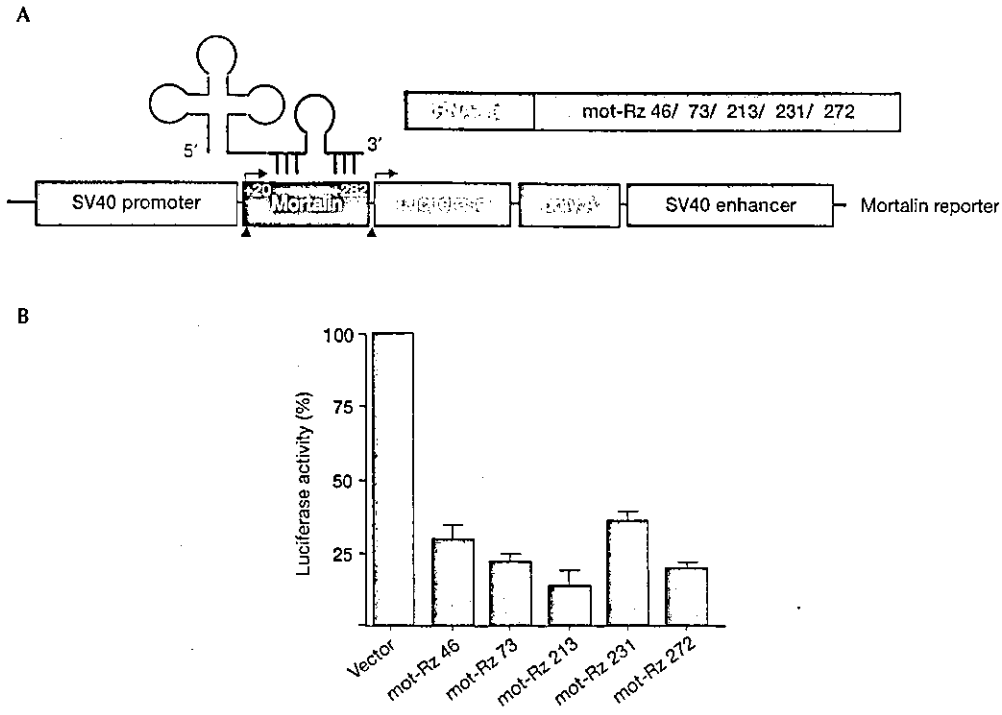

Fig. 2 | Effect of mortalin ribozymes on the expression of a mortalin–luciferase reporter. (A) Schematic representation of the mortalin–luciferase reporter expression plasmid, which is driven by the simian virus 40 (SV40) promoter. The target sites of the mortalin ribozymes (mot-Rzs) were at nucleotide residues 46, 73, 213, 231 and 272, as shown in Fig. 1. (B) Luciferase reporter activity in cells transfected with mortalin–luciferase and mot-Rzs. Cells were lysed 48 h after transfection, and were assayed as described in the Methods section. tRNA, transfer RNA.

itself was visualized instead of the reporter protein or its activity, was performed as shown in Fig. 3. An expression plasmid that encoded a V5-epitope-tagged N-terminal region of the mortalin protein (amino-acid residues 1–435) was co-transfected with the mot-Rz constructs, as described in the Methods section. The effectiveness of the mot-Rzs was determined by the visualization of the mortalin–V5 protein by western blotting with an anti-V5 antibody (Fig. 3B). As mot-Rz 46 and mot-Rz 73 have target sites in the 5′ upstream non-coding region (Fig. 1), these could not be used for this assay. mot-Rz 213 and mot-Rz 231 have overlapping targeting sites; mot-Rz 213 was more effective in luciferase assays (Figs 1,2). Thus, mot-Rz 213 and mot-Rz 272 were used for this direct assay for mortalin suppression. Both the ribozymes caused a significant reduction of mortalin–V5 protein levels. A titration experiment, in which different amounts of the mot-Rz 213 plasmid and a constant amount of the mortalin–V5 reporter-plasmid were transfected, showed a dose-dependent decrease in mortalin–V5 protein levels. Transfection efficiencies were normalized by the co-transfection of a green fluorescent protein (GFP) reporter plasmid. Protein loading was normalized by western blotting using an anti-actin antibody. These data showed that mot-Rzs have sufficient catalytic activity, and could thus be used for the suppression of the expression of endogenous mortalin in cells.

Next, we transfected mot-Rzs into human fibrosarcoma (HT1080) cells. Transfected cells were selected in medium supplemented with puromycin (2.5 μg ml^{-1}) for 3–5 days. The selected cells were maintained in medium supplemented with 0.5–1.0 μg ml^{-1} puromycin, and the pooled cultures were analysed for endogenous mortalin expression by northern and western blotting. Surprisingly, and in contrast to our expectations, none of the mot-Rzs caused any significant decrease of the endogenous levels of the protein (Fig. 4A); the mortalin transcript seemed to be affected only slightly. There are two possible interpretations of this data: first, the ribozymes may not have been expressed at sufficiently high levels in these cells; or second, the expressed ribozymes may not be active against the endogenous mortalin transcript, possibly due to inaccessibility of the target (Fig. 1A). To examine the first possibility, we analysed the expression of the mot-Rzs by RT–PCR (PCR after reverse transcription) and northern blotting, and found that the mot-Rzs were expressed (Fig. 4B), but at varying levels. To investigate the second possibility, we used recently developed RNA-helicase-linked hybrid ribozymes (HyRzs; Warashina *et al.*, 2001; Kawasaki & Taira, 2002), as described below.

RNA-helicase-linked hammerhead ribozymes for mortalin

HyRzs coupled to RNA helicase were found to have a substrate-unwinding activity that improves their ability to access targets, as shown schematically in Fig. 5A. Poly(A)-linked RNA-helicase-recruiting mortalin ribozymes were therefore constructed as described in the Methods section. For a direct comparison, the target sites used were the same as those used for the conventional mot-Rzs (Fig. 1). First, the catalytic activity of these ribozymes was examined using a mortalin–luciferase reporter plasmid construct, as described in the Methods section. All four of the mortalin HyRzs suppressed the activity of the mortalin–luciferase reporter effectively (Fig. 5B). HT1080 cells were stably transfected with these HyRzs, and were selected in medium supplemented with puromycin. Many of the colonies (60–70%) in cells transfected with HyRz 231 and HyRz 272 seemed to be growth arrested as compared with cells transfected with

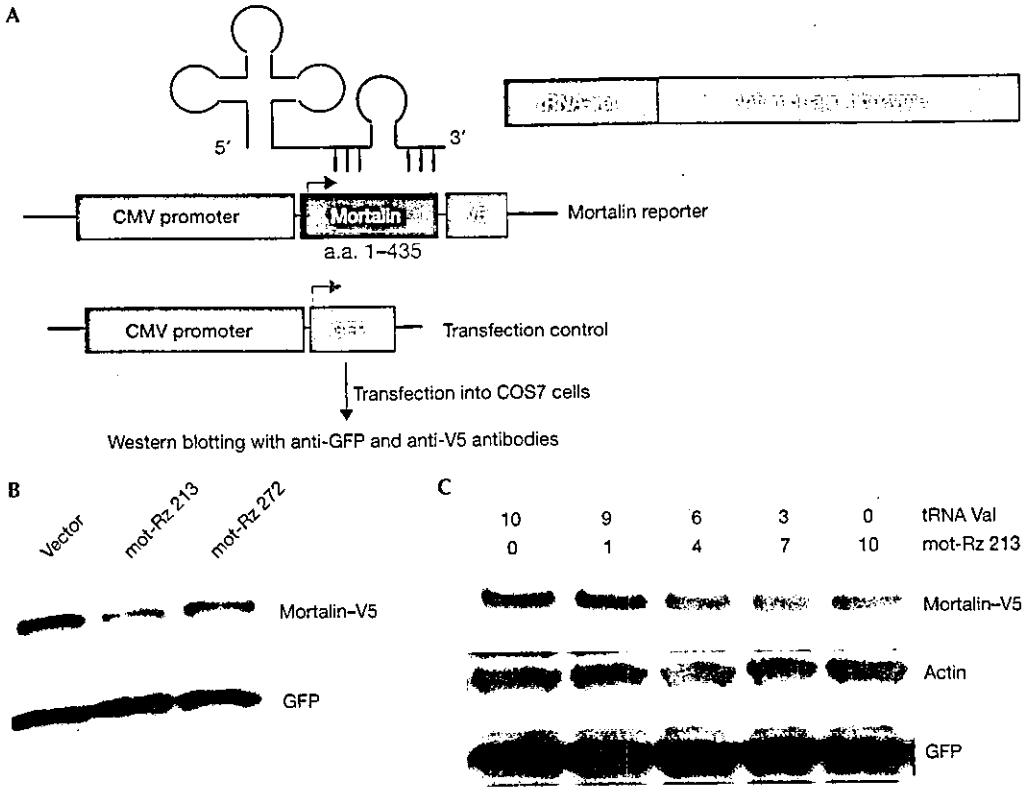

Fig. 3 | Effect of mortalin ribozymes on the expression of the mortalin–V5 reporter. (A) Schematic representation of an expression plasmid encoding a mortalin–V5 protein that is driven by the cytomegalovirus (CMV) promoter. The expression of green fluorescent protein (GFP) driven by the CMV promoter was used as a control for transfection efficiency. (B) Western blotting from cells transfected with the mortalin–V5 reporter and the indicted mortalin ribozymes (mot-Rzs). Cells were lysed 48–72 h after transfection, and the lysates were western blotted using an anti-V5 antibody. (C) Western blotting from cells transfected with the mortalin–V5 reporter and varying amounts of mot-Rz 213. GFP and actin were used as transfection and loading controls, respectively. a.a., amino acids; tRNA, transfer RNA.

vector only, HyRz 73 or HyRz 213. The level of expression of endogenous mortalin was analysed in selected pooled cultures by western blotting with an anti-mortalin antibody. Cells transfected with HyRz 231 or HyRz 272 showed lower levels of mortalin expression than vector-only-transfected cells (Fig. 5C). Cells transfected with HyRz 73 or HyRz 213 showed a significant reduction in the activity of the mortalin–luciferase reporter (Fig. 5B), but there was no reduction in endogenous mortalin expression (Fig. 5C). This suggests that there is a complex mortalin mRNA structure and that the target sites are inaccessible, even in the presence of coupled helicase activity. Interestingly, cultures transfected with any of the conventional ribozymes or with HyRz 73 and HyRz 213 did not show the growth arrest observed in HyRz-231- and HyRz-272-transfected cultures. Next, we isolated colonies that seemed to be growth arrested from HT1080 cultures that were transfected with HyRz 231 and HyRz 272 (Fig. 6A). Whereas vector-only-transfected cells rapidly formed dense colonies, cells transfected with HyRz 231 or HyRz 272 had a slow growth rate and a flattened morphology (Fig. 6A). Analysis of mortalin expression in these colonies by western blotting revealed a significant decrease in expression compared with the untransfected and vector-only-transfected cells (Fig. 6B). The colonies were maintained in culture for at least nine weeks. These colonies continued to show slow growth and a rather flattened morphology compared with the untransfected and vector-only-transfected cells (Fig. 6A), suggesting that the proliferation rate of cells depends on the level of mortalin expression. These data showed that, whereas conventional mot-Rzs were ineffective, the RNA-helicase-coupled HyRzs, targeted to the same sites, caused suppression of mortalin expression. This indicates that the mortalin transcript has a structure that is not easily accessible to the conventional mot-Rzs. The novel RNA-helicase-coupled HyRzs were effective in this case, resulting in reduced mortalin expression and growth arrest of transformed cells.

Many immortal and transformed human cell lines have higher levels of mortalin expression than their normal counterparts (Takahashi *et al.*, 1994; Bini *et al.*, 1997; Kaul *et al.*, 1998). The exogenous expression of human mortalin (MOT2) caused the malignant transformation of NIH 3T3 cells (Kaul *et al.*, 1998) and lifespan extension of normal human fibroblasts (Kaul *et al.*, 2000), possibly by mechanisms involving the inactivation of the tumour suppressor protein p53 (Kaul *et al.*, 2001; Wadhwa *et al.*, 1998, 2002c) and other proteins that are thought to involve its mitochondrial import and chaperone functions (Liu *et al.*, 2001; Wadhwa *et al.*, 2002a,b). To determine whether the growth arrest of transformed cells by the targeting of mortalin was caused by the abrogation of its p53-inactivation function, we performed p53-dependent reporter assays in U2OS/PG13Luc cells (U2OS cells that are stably transfected with a p53-dependent luciferase reporter) that express wild-type p53. Cells transfected with HyRz 231 and HyRz 272 showed a 2–3-fold higher level

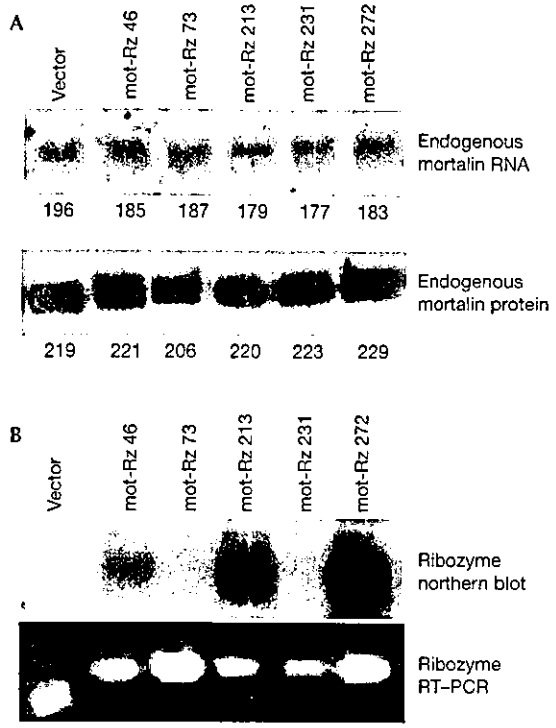

Fig. 4 | Endogenous mortalin expression in cells transfected with mortalin ribozymes. (A) Northern blot (upper panel) and western blot (lower panel) analyses of cells transfected with vector only or with the mortalin ribozyme (mot-Rz) expression plasmids indicated. The numbers below the lanes indicte relative units of mortalin expression. (B) Expression analysis of mot-Rzs by northern blotting (upper panel) and RT–PCR (PCR after reverse transcription; lower panel).

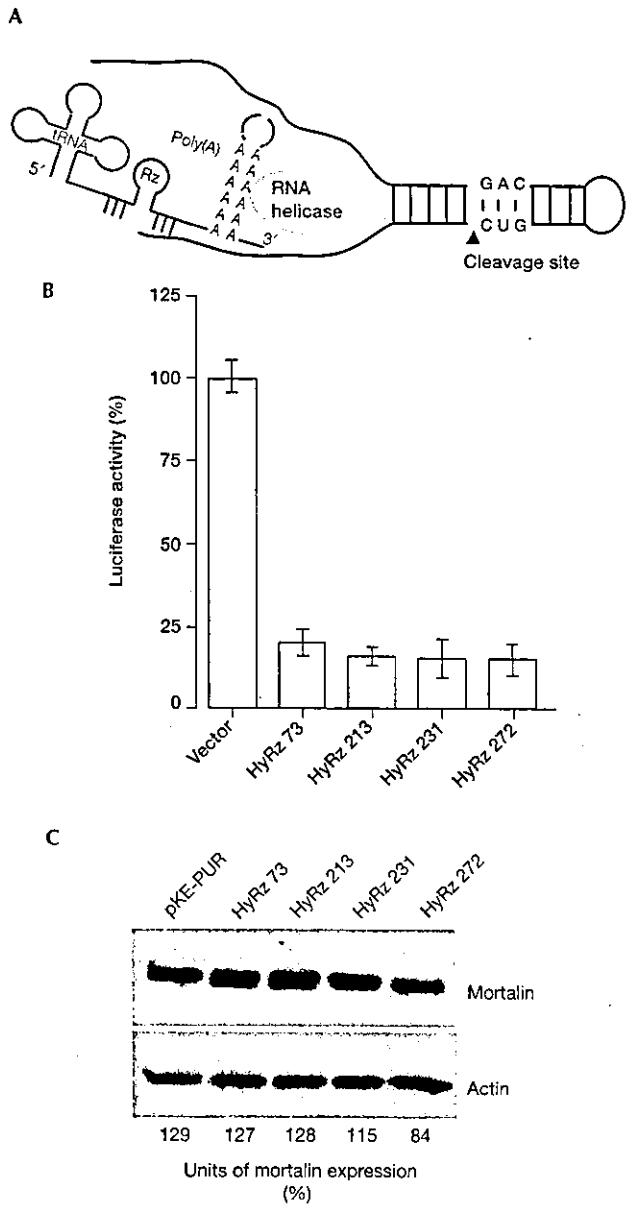

Fig. 5 | RNA-helicase-coupled ribozymes targeted against mortalin. (A) Schematic representation of RNA-helicase-coupled hammerhead ribozymes (HyRzs). The poly(A) sequence recruits RNA helicase, which uncoils the target transcript and improves the accessibility of the HyRz to the target sites. (B) Effects of mortalin HyRzs in a mortalin–luciferase reporter assay. Cells were lysed 48–72 h after transfection, and were assayed for luciferase activity as described in the Methods section. (C) Endogenous mortalin expression in cells that were transfected with mortalin HyRzs and selected in puromycin-supplemented medium. Cells transfected with HyRz 231 and HyRz 272 showed a reduction in mortalin expression. Western blots were scanned using a Micro Computer Imaging Device (MCID-M2; FUJIX). The ratios of the mortalin signals to the actin signals are shown as relative units of mortalin expression. Rz, ribozyme; tRNA, transfer RNA.

of p53 activity than vector-only-transfected and HyRz-272-transfected cells, suggesting that p53 function is activated as a result of targeting mortalin. Such activation of p53 function may account for the growth arrest of cells expressing wild-type p53. To examine further the effect of mortalin targeting on the long-term proliferative ability of cells, we performed colony-forming-efficiency assays. The following cells, which have variable statuses with respect to wild-type p53, were used: HT1080 (partial loss of p53 expression); U2OS (wild-type p53); Saos-2 (complete loss of p53); and MCF7 (wild-type p53). These were transfected with vector only, HyRz 231, HyRz 272 and an inactive version of an unrelated ribozyme, which was made against the peroxisomal protein Pex19; Wadhwa *et al.*, 2002d). Mortalin-specific HyRzs decreased colony-forming efficiency as compared with the vector and the inactive ribozyme (Fig. 6C; and data not shown). Furthermore, cells that expressed wild-type p53 (HT1080, U2OS and MCF7) showed stronger suppression of colony-forming efficiency than the p53-null (Saos-2) cells (data not shown). This data suggests that the growth arrest involves the activation of p53 and p53-independent pathways. This may involve mitochondrial import and chaperone functions of mortalin, as suggested by other studies (Liu *et al.*, 2001; Wadhwa *et al.*, 2002a,b). On the basis of these data, the targeting of mortalin could be used as a tool for cancer therapy. We have shown here for the first time that such targeting is possible using RNA-helicase-coupled hybrid ribozymes, a powerful tool for targeting gene expression *in vivo*.

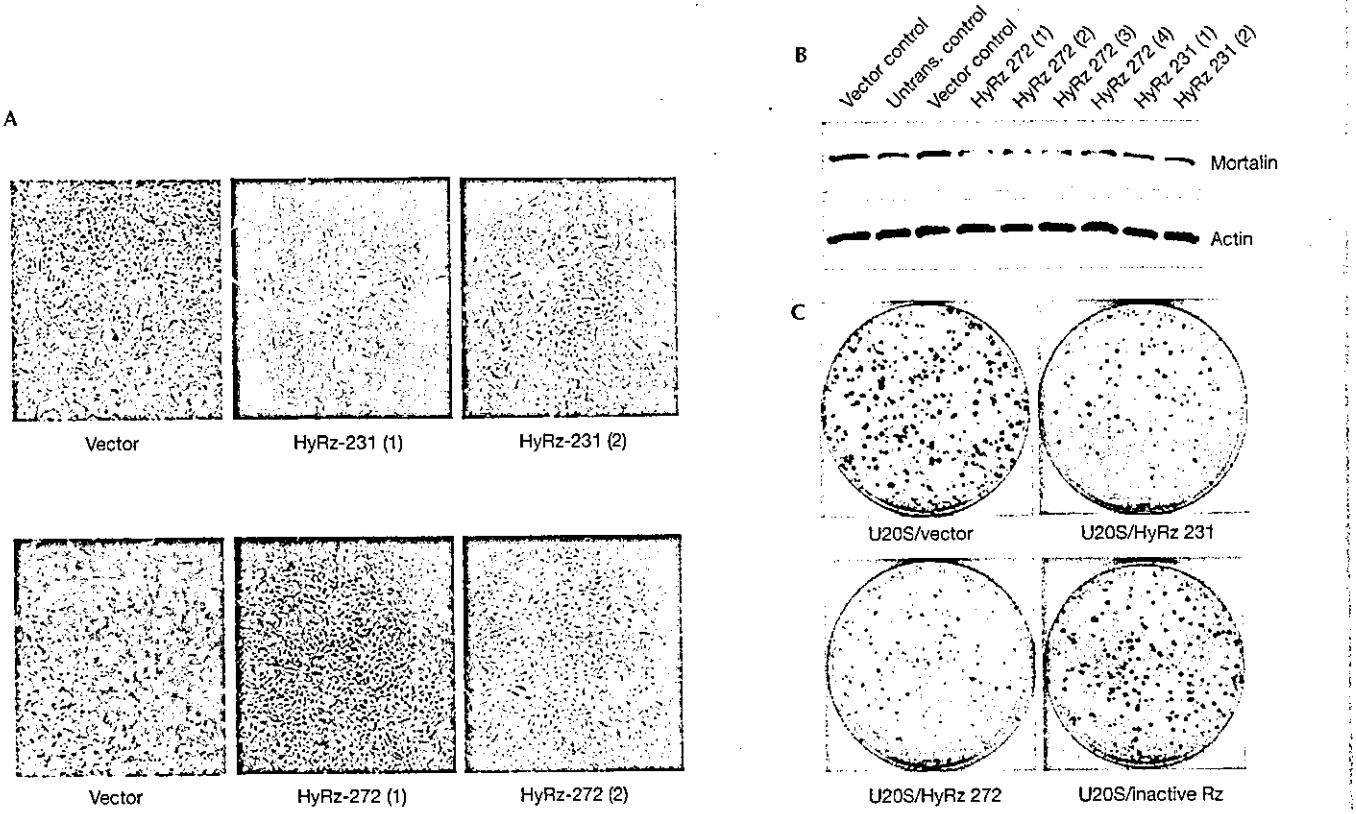

Fig. 6 | Effect of RNA-helicase-coupled ribozymes targeted against mortalin on cell growth and mortalin expression levels. (A) Phase-contrast images of human fibrosarcoma HT1080 cell clones transfected with vector only or with the RNA-helicase-coupled ribozymes (HyRzs) HyRz 231 and HyRz 272. Cells transfected with vector only grew quickly to form dense, shiny colonies. Cells transfected with HyRz 231 and HyRz 272 grew slowly, and had a flattened morphology. (B) Endogenous mortalin expression in clones selected from cells transfected with vector only, HyRz 231 or HyRz 272. HyRz-transfected clones showed low levels of mortalin expression. Actin was used as a loading control. (C) Colony-forming efficiency assay of U2OS cells transfected with empty vector, HyRz 231, HyRz 272 or an inactive, unrelated ribozyme. Suppression of colony formation was seen only in cells transfected with HyRz 231 and HyRz 272. Untrans., untransfected.

METHODS

Construction of RNA-polymerase-III-driven hammerhead-ribozyme expression plasmids. Target sites flanking the ten putative ribozyme cleavage sites (GUC, GUA, CUC and CUA) in the 5′ region of the mortalin complementary DNA sequence were selected. A partial secondary structure of mortalin RNA (Fig. 1A), and structures of each of the target sites, the ribozyme and the transfer-RNA sequence (155 nucleotides; Fig. 1B) were predicted using the Mfold programme (ftp://iubio.bio.indiana.edu/molbio/mac/mulfold.hqx; Zuker, 1989). Five target sites (with cleavage sites at nucleotides 46, 73, 213, 231 and 272; Fig 1B, shown in red) that had at least a 60% open structure (Fig. 1B) when embedded in ribozyme and tRNA sequences were selected, and were constructed in the pKE-PUR vector, as described in Koseki *et al.* (1999; Fig. 1C). The DNA oligonucleotide (TCCCCG GTTCGAAACCGGGCACTACAAAAACCAACTTTXXXXXXXXXCT GATGAGGCCGAAAGGCCGAAXXXXXXXXXGGTACCCCG GATATCTTTTTTT), which comprises the tRNA sequence, the ribozyme sequence (flanked by the gene-targeting sequence (X_9)), and the linker sequence, was synthesized. This oligonucleotide was made by PCR, using the upper-strand primer 5′-TCCCCGGTTCGAAAC CGGGCACTAC-3′ and the lower-strand primer 5′-AGAAAAAAA GATATCCGGGGTACC-3′, with 25 cycles of 94 °C for 30 s, 58 °C for 30 s, and 72 °C for 45 s. The product was purified, cut with *Csp*45I and *Kpn*I, and ligated into the pPUR-KE vector (Kato *et al.*, 2001). The empty vector, which contained the tRNA sequence but no ribozyme, was used as a negative control.

Construction of mortalin reporter plasmids. Two kinds of mortalin reporter plasmids were constructed. The first consisted of a mortalin–luciferase reporter driven by the simian virus 40 promoter. Mortalin amino-acid residues 20–282 were fused to the N-terminus of luciferase (Fig. 2A). The reporter activity was determined by luciferase assays. The second mortalin reporter plasmid encoded the N-terminal region of mortalin tagged with a V5 epitope at its carboxyl terminus (Fig. 3A) under the control of the cytomegalovirus promoter (provided by the pCDNA3.1 vector, Invitrogen). The reporter activity was determined by western blotting using an anti-V5 antibody (Invitrogen).

Cell culture, transfections and colony-forming assays. HT1080, osteosarcoma (U2OS and Saos-2), breast carcinoma (MCF7) and monkey kidney (COS7) cells were cultured in a humidified incubator in DMEM supplemented with 10% FBS, penicillin, streptomycin and fungizone (Life Technologies, Inc.) at 37 °C in the presence of 5% CO_2.

Transfections were performed using Lipofectamine PLUS (Invitrogen). Usually, 3 or 8 μg of plasmid DNA was used for each 6-cm or 10-cm dish, which contained cells at 60% confluence. Cells were selected in medium supplemented with puromycin (2.5 μg ml^{-1}) for 3–5 days, and were then cultured in

the presence of 0.5–1 μg ml^{-1} puromycin. For colony-forming assays, 1,000 cells were plated in 10-cm dishes and were monitored until the appearance of colonies (10–14 days). Colonies were washed with PBS, fixed with methanol:acetone (1:1) and stained with 0.1% aqueous crystal violet (Sigma).

Luciferase reporter assay. Cells were transfected with the mortalin–luciferase reporter plasmid and the mot-Rzs. Cells were then selected in medium supplemented with puromycin (2.5 μg ml^{-1}) for 2–4 days, and were then maintained in medium lacking puromycin for at least 24–48 h. Luciferase assays were performed using a Dual-Luciferase Reporter Assay System (Promega).

Northern blotting. Total RNA was prepared from cells at 70% confluence in 10-cm dishes using Trizol (Life Technologies, Inc.). The RNA was denatured and fractionated according to size using 1% agarose gels containing 2.2 M formaldehyde, and was then transferred to a Hybond N+ membrane (Amersham Biosciences). 1.6-kb fragments of the human mortalin cDNA or the ribozyme sequence were used as probes for determining the expression levels of mortalin and ribozyme, respectively. Hybridization was performed at 65 °C in express hybridization buffer (Clontech). The membrane was washed for 10 min in each of 2 × SSC and 2 × SSC, 0.1% SDS, and was then washed twice in 1 × SSC and 0.1% SDS, followed by autoradiography. The amount of RNA loaded was determined by hybridization of the blots with an actin probe.

Detection of ribozyme expression by RT–PCR. RT–PCR was carried out on total RNA (2 μg) prepared from cells transfected with the ribozyme plasmids or with empty vector (as a control). The RNA was reverse-transcribed using the lower-strand primer described below and Moloney murine leukaemia virus reverse transcriptase (at 42 °C for 90 min). The reverse-transcribed product was then amplified by PCR using the upper-strand primer 5′-TCCCCGGTTCGAAAC CGGGCA-3′ and the lower-strand primer 5′-GCTTGCATGCCT GCAGGTCGACGCGATAGAAAAAAAGATATCCGGGGT-3′ for 20 cycles at 94 °C, 52 °C and 72 °C for 30 s each. The amplified product (100 bp) was run on a 2.6% agarose gel and visualized by ethidium bromide staining.

Western blot analysis. Protein samples (10–20 μg) were separated on SDS–polyacrylamide gels and electroblotted onto nylon membranes (Millipore) using a semi-dry-transfer apparatus. Immunoassays were performed with polyclonal anti-mortalin (Wadhwa *et al.*, 1993) or anti-actin (MAB1501R; Chemicon) antibodies. The immunocomplexes formed were visualized with horseradish-peroxidase-conjugated secondary antibodies using an enhanced chemiluminescence kit (Amersham Biosciences).

ACKNOWLEDGEMENTS

We thank T. Yaguchi for excellent technical assistance. The study was partly supported by NEDO Research Grants, Japan.

REFERENCES

Akashi, H., Kawasaki, H., Kim, W.J., Akaike, T., Taira, K. & Maruyama, A. (2002) Enhancement in the cleavage activity of a hammerhead ribozyme by cationic comb-type polymers and an RNA helicase *in vitro*. *J. Biochem.*, **131**, 687–692.

Bini, L. *et al.* (1997) Protein expression profiles in human breast ductal carcinoma and histologically normal tissue. *Electrophoresis*, **18**, 2832–2841.

Cech, T.R. (1986) Biologic catalysis by RNA. *Harvey Lect.*, **82**, 123–144.

Cech, T.R. (2000) Structural biology. The ribosome is a ribozyme. *Science*, **289**, 878–879.

Cech, T.R. & Uhlenbeck, O.C. (1994) Ribozymes. Hammerhead nailed down. *Nature*, **372**, 39–40.

Doudna, J.A. & Cech, T.R. (2002) The chemical repertoire of natural ribozymes. *Nature*, **418**, 222–228.

Hammann, C. & Lilley, D.M. (2002) Folding and activity of the hammerhead ribozyme. *Chembiochem*, **3**, 690–700.

Kato, Y., Kuwabara, T., Warashina, M., Toda, H. & Taira, K. (2001) Relationships between the activities *in vitro* and *in vivo* of various kinds of ribozyme and their intracellular localization in mammalian cells. *J. Biol. Chem.*, **276**, 15378–15385.

Kaul, S.C., Duncan, E.L., Englezou, A., Takano, S., Reddel, R.R., Mitsui, Y. & Wadhwa, R. (1998) Malignant transformation of NIH3T3 cells by overexpression of mot-2 protein. *Oncogene*, **17**, 907–911.

Kaul, S.C., Reddel, R.R., Sugihara, T., Mitsui, Y. & Wadhwa, R. (2000) Inactivation of p53 and life span extension of human diploid fibroblasts by mot-2. *FEBS Lett.*, **474**, 159–164.

Kaul, S.C., Reddel, R.R., Mitsui, Y. & Wadhwa, R. (2001) An N-terminal region of mot-2 binds to p53 *in vitro*. *Neoplasia*, **3**, 110–114.

Kawasaki, H. & Taira, K. (2002) Identification of genes by hybrid ribozymes that couple cleavage activity with the unwinding activity of an endogenous RNA helicase. *EMBO Rep.*, **3**, 443–450.

Kawasaki, H., Ohkawa, J., Tanishige, N., Yoshinari, K., Murata, T., Yokoyama, K.K. & Taira, K. (1996) Selection of the best target site for ribozyme-mediated cleavage within a fusion gene for adenovirus E1A-associated 300 kDa protein (p300) and luciferase. *Nucleic Acids Res.*, **24**, 3010–3016.

Koseki, S., Tanabe, T., Tani, K., Asano, S., Shioda, T., Nagai, Y., Shimada, T., Ohkawa, J. & Taira, K. (1999) Factors governing the activity *in vivo* of ribozymes transcribed by RNA polymerase III. *J. Virol.*, **73**, 1868–1877.

Kuwabara, T., Warashina, M., Koseki, S., Sano, M., Ohkawa, J., Nakayama, K. & Taira, K. (2001) Significantly higher activity of a cytoplasmic hammerhead ribozyme than a corresponding nuclear counterpart: engineered tRNAs with an extended 3′ end can be exported efficiently and specifically to the cytoplasm in mammalian cells. *Nucleic Acids Res.*, **29**, 2780–2788.

Kuwabara, T., Warashina, M. & Taira, K. (2002) Cleavage of an inaccessible site by the maxizyme with two independent binding arms: an alternative approach to the recruitment of RNA helicases. *J. Biochem.*, **132**, 149–155.

Liu, Q., Krzewska, J., Liberek, K. & Craig, E.A. (2001) Mitochondrial Hsp70 Ssc1: role in protein folding. *J. Biol. Chem.*, **276**, 6112–6118.

Miyagishi, M., Kuwabara, T. & Taira, K. (2001) Transport of intracellularly active ribozymes to the cytoplasm. *Cancer Chemother. Pharmacol.*, **48**, S96–S101.

Pyle, A.M. (2002) Metal ions in the structure and function of RNA. *J. Biol. Inorg. Chem.*, **7**, 679–690.

Takagi, Y., Warashina, M., Stec, W.J., Yoshinari, K. & Taira, K. (2001) Survey and summary: recent advances in the elucidation of the mechanisms of action of ribozymes. *Nucleic Acids Res.*, **29**, 1815–1834.

Takahashi, S. *et al.* (1994) Correlation of heat shock protein 70 expression with estrogen receptor levels in invasive human breast cancer. *Am. J. Clin. Pathol.*, **101**, 519–525.

Wadhwa, R., Kaul, S.C., Ikawa, Y. & Sugimoto, Y. (1993) Identification of a novel member of mouse hsp70 family. Its association with cellular mortal phenotype. *J. Biol. Chem.*, **268**, 6615–6621.

Wadhwa, R., Takano, S., Robert, M., Yoshida, A., Reddel, R.R., Nomura, H., Mitsui, Y. & Kaul, S.C. (1998) Inactivation of tumor suppressor p53 by mot-2, an hsp70 family member. *J. Biol. Chem.*, **273**, 29586–29591.

Wadhwa, R., Taira, K. & Kaul, S.C. (2002a) An hsp70 family chaperone, mortalin/mthsp70/PBP74/Grp75: what, when and where? *Cell Stress Chaperones*, **7**, 309–316.

Wadhwa, R., Taira, K. & Kaul, S.C. (2002b) Mortalin: a potential candidate for biotechnology and biomedicine. *Histochem. Histopathol.*, **17**, 1173–1177.

Wadhwa, R., Yaguchi, T., Hasan, M.K., Mitsui, Y., Reddel, R.R. & Kaul, S.C. (2002c) Hsp70 family member, mot-2/mthsp70/GRP75, binds to the cytoplasmic sequestration domain of the p53 protein. *Exp. Cell Res.*, **274**, 246–253.

Wadhwa, R., Sugihara, T., Hasan, M.K., Taira, K., Reddel, R.R. & Kaul, S.C. (2002d) A major functional difference between the mouse and human ARF tumor suppressor proteins. *J. Biol. Chem.*, **277**, 36665–36670.

Warashina, M., Kuwabara, T., Kato, Y., Sano, M. & Taira, K. (2001) RNA–protein hybrid ribozymes that efficiently cleave any mRNA independently of the structure of the target RNA. *Proc. Natl Acad. Sci. USA*, **98**, 5572–5577.

Yarus, M. (1999) Boundaries for an RNA world. *Curr. Opin. Chem. Biol.*, **3**, 260–267.

Zhang, B. & Cech, T.R. (1997) Peptide bond formation by *in vitro* selected ribozymes. *Nature*, **390**, 96–100.

Zuker, M. (1989) On finding all suboptimal foldings of an RNA molecule. *Science*, **244**, 48–52.